

Warped Universal Extra Dimensions

Aníbal D. Medina ^a and Eduardo Pontón ^b

^a*Department of Physics, University of California, One Shields Ave. Davis, CA 95616, USA*

^b*Department of Physics, Columbia University, 538 W. 120th St, New York, NY 10027, USA*

April 22, 2022

Abstract

We consider a 5D warped scenario with a KK-parity symmetry, where the non-trivial warping arises from the dynamics that stabilizes the size of the extra dimension. Generically, the lightest Kaluza-Klein (KK) particle is the first excitation of the radion field, while the next-to-lightest Kaluza-Klein particle is either the first excitation of the (RH) top quark or the first KK-parity odd Higgs. All these masses are expected to be of order the electroweak scale. We present simple analytical expressions for the masses and wavefunctions of the lowest lying KK modes, and derive the Feynman rules necessary for phenomenological applications. The framework allows to interpolate between a strongly warped scenario á la Randall-Sundrum (RS), and a weakly warped scenario that shares properties of both RS and Universal Extra Dimensions models.

1 Introduction

Warped extra dimensional scenarios provide an appealing solution to the hierarchy problem [1]. In addition, when the SM gauge bosons [2, 3] and fermions [4] arise from higher-dimensional fields one gains a rather interesting understanding of the SM fermion hierarchies and CKM mixing angles, based on the localization of these modes along the extra dimension [5]: light fermion fields are localized near the “UV brane” while heavier fermions, most notably the top quark, are localized closer to the “IR brane”. At the same time dangerous flavor-changing neutral current effects are suppressed, and can be roughly consistent with low-energy constraints even when the new physics is at the TeV scale. The associated spectrum of Kaluza-Klein (KK) modes provides exciting signals at the LHC.

It was recognized early on [6, 7] that a complete solution to the hierarchy problem requires the specification of dynamics that stabilizes the size of the extra dimensions. In the Randall-Sundrum (RS) scenario [1], this requires that the interbrane separation be stabilized at a factor of ~ 35 in units of the inverse curvature scale. This can be achieved either at tree-level, by considering for example a SM singlet scalar that acquires a non-trivial vacuum expectation value (VEV) [8], or at the quantum level (see e.g. [9, 10, 11, 12, 13, 14]). An important consequence is the presence of a 4D scalar mode, called the “radion”, that corresponds to the fluctuations in the interbrane distance. The radion mode is expected to be parametrically lighter than the KK states, and therefore potentially important in the phenomenology of these scenarios. The generic couplings of the radion to SM fields were worked out in Refs. [15, 16, 17, 18]. Except for a possible mixing term with the Higgs field [19, 20, 21], these interactions are non-renormalizable and suppressed by a “radion decay constant”, Λ_r .

In this paper we propose stabilizing the size of the extra-dimension, parameterized by $y \in [-L, L]$, in such a way that the non-trivial warping arises from the backreaction of a Goldberger-Wise (GW) scalar, with the geometry being symmetric about $y = 0$. As a result, the boundaries of the space, at $y = \pm L$, are IR boundaries where the warp factor is smallest, while the maximum of the warp factor is achieved at $y = 0$. Thus, although no UV brane is put in by hand, a dynamical “UV brane” is generated in the middle of the extra dimension. In fact, in a certain limit this UV brane becomes infinitely thin, and the framework reduces to two copies of the RS scenario [1] glued together at the UV brane, as considered in [22]. However, generically, the dynamical UV brane is “fat”, and the geometry is not simply AdS_5 .

One important consequence of the setup, that goes beyond the most studied implementations of the RS proposal (for a review, see e.g. [23]), is the existence of a discrete Z_2 symmetry under which all the even-level KK states (which include the zero-modes) are Z_2 -even, while the odd-level modes are Z_2 -odd (i.e. a KK parity similar to the one present in Universal Extra Dimensional scenarios or UED’s [24, 25]). As a result, the lightest KK-parity odd particle (the LKP) is stable, and a potential dark matter (DM) candidate (for an alternative proposal, see [26]). However, unlike in UED scenarios [27, 28], the KK states are *not necessarily* highly degenerate, with the degeneracy broken by loop-level effects, but instead larger mass splittings can be expected (although there are some interesting degeneracies, related to localization effects). A similar idea of a warped framework with a KK parity was explored in [22], where the viability of the first KK excitation of the Z gauge boson as a DM

candidate was investigated. Here, we point out that the LKP is generically expected to be the first KK excitation of the radion field (more precisely of the radion/GW-scalar system). We show that its mass is highly degenerate with the radion mass, and that its interactions are also controlled by Λ_r . Then, the question of the viability of the first KK radion as a DM candidate naturally arises, and answering it becomes essential in such warped frameworks with a KK parity. The point is that, although it is expected that the LKP has a mass of order the EW scale, its interactions may not be sufficiently strong to ensure the annihilation of KK radions during the early history of the universe to levels below the “overclosure limit”. The WIMP miracle is not necessarily automatic, and the danger of overproducing the LKP’s becomes a pressing issue. Fortunately, there are a number of scenarios one can envision where the KK radion relic density can be suppressed and explain the observed DM density. We explore these in detail in the companion paper [29].

In this work we lay out the formalism necessary to analyze the properties of the LKP, which includes also a discussion of the KK excitations of fermion and gauge fields. Since we consider a rather general gravitational background, it is difficult to find closed solutions for the KK wavefunctions. However, we obtain reasonably accurate analytical approximation for the lightest states in the theory, which include the radion, the KK radion and possibly the first KK excitation of the (RH) top. These become more accurate in the limit that the UV brane is fat, which corresponds to an interesting deformation of the RS proposal. We also point out that fermion zero-mode localization is naturally achieved by coupling the 5D fermions to the GW scalar that induces the warping and stabilizes the size of the extra dimension. Thus, no ad-hoc 5D fermion masses need to be introduced. Regarding the EWSB sector, it is shown that it is naturally a two-Higgs doublet model (THDM), with the second doublet being a KK-parity odd excitation of the SM Higgs.

Our formalism also allows us to interpolate between a strongly warped limit (à la RS) and a limit where the curvature is small, which is similar to the UED assumption. An interesting intermediate case arises when the curvature is small compared to the 5D Planck mass, but not exactly zero. In this case, the hierarchy between the Planck and the electroweak (EW) scales arises in part from a moderate warp factor, and in part from the smallness of the curvature scale. Such a scenario can share phenomenological properties of both RS and UED scenarios. It can also give rise to KK radion DM as a non-thermal relic [29]. Our approach is somewhat different from the recently studied “soft-wall” scenarios [30]–[39], but it could be interesting to combine the two ideas to obtain a fully dynamical warped compactification.

The outline of this work is as follows: in Section 2 we give several examples that illustrate the stabilization of the extra dimension with an automatic KK-parity symmetry. We explore various limits, imposing a minimal number of phenomenological constraints, and define two benchmark scenarios to be used as reference. In Section 3, we discuss the KK decomposition of the radion/GW-scalar system, thus defining the radion decay constant Λ_r . We also give simple analytical expressions for the mass and wavefunction profiles of both the radion and its first KK excitation (the LKP). Section 4 is devoted to a study of fermions in the Z_2 symmetric backgrounds. We point out that in the fat UV brane limit it is possible to characterize the localization of the zero-mode via a dimensionless c -parameter that is analogous to the treatment in the pure AdS₅ background, although there are important

differences. We also give approximate analytical expressions for the mass and wavefunction of the first fermion KK resonance in cases where it is parametrically lighter than the KK scale (hence the likely next-to-lightest KK-parity odd particle, or NLKP). Section 5 is devoted to bulk scalars as applied to the Higgs field. We also present the Higgs Yukawa interactions with bulk fermions. Gauge fields are briefly discussed in Section 6. In preparation to the DM analysis to be presented in [29], we work out in Section 7 the Feynman rules for the interactions between the radion/KK-radion and the KK fermions, gauge bosons and the Higgs doublets. We summarize and conclude in Section 8.

2 General Setup

In this section we describe the stabilization mechanism that leads to a non-trivial Z_2 -symmetric warping. We illustrate this by choosing scalar potentials that allow for closed analytical solutions that take into account the scalar backreaction on the metric, but emphasize that the properties we are interested in do not depend on any given particular choice of potential. We discuss an initial set of phenomenological constraints, and define two benchmark scenarios, one with strong warping and one where the curvature is small compared to the 5D Planck scale.

2.1 Backgrounds with Z_2 Symmetry

We start with a 5D real scalar Φ minimally coupled to gravity according to

$$S = \int_M d^5x \sqrt{g} \left[-\frac{1}{2} M_5^3 \mathcal{R}_5 + \frac{1}{2} \nabla_M \Phi \nabla^M \Phi - V(\Phi) \right] + \int_{\partial M} d^4x \sqrt{g_{\text{ind}}} \mathcal{L}_4(\Phi) , \quad (1)$$

where M_5 is the (reduced) 5D Planck mass, \mathcal{R}_5 is the 5D Ricci scalar, and the last term allows for operators localized on the boundary of the fifth dimension (which will be specified in the next subsection). We assume that the fifth dimension is compactified to an interval, parameterized by $y \in [-L, L]$. Our interest is in dynamics that stabilizes the size of the extra dimensions, $2L$, while leading to a background that is symmetric about $y = 0$, so that a geometric Z_2 symmetry¹ is present, as in [22]. However, unlike Ref. [22] we do not have a central brane at $y = 0$, although as we will see, in certain limits, such a brane arises from the scalar dynamics.

We are interested in solving for the coupled gravity/scalar system, taking into account the backreaction of a scalar VEV on the geometry, since this results in the stabilization of the extra dimension à la Goldberger-Wise [8]. We restrict to backgrounds exhibiting 4D Lorentz symmetry, which can always be put in the form

$$ds^2 = e^{-2A(y)} \eta_{\mu\nu} dx^\mu dx^\nu - dy^2 , \quad (2)$$

¹As established in [40], Chern-Simons terms do not break the KK-parity symmetry, so that the questions raised in [41] for little Higgs scenarios with T-parity do not apply.

where y is the proper distance. The weak energy condition implies that $A''(y) \geq 0$ [42] so that $e^{-A(y)}$ must be a convex function and the two boundaries at $y = \pm L$ are IR branes in the RS terminology. As shown in Refs. [43, 44], Einstein's equations, together with the scalar equation of motion, can be solved exactly for the class of scalar potentials given by

$$V(\Phi) = \frac{1}{8} \left(\frac{\partial W(\Phi)}{\partial \Phi} \right)^2 - \frac{1}{6M_5^3} W(\Phi)^2, \quad (3)$$

where $W(\Phi)$ is an arbitrary ‘‘superpotential’’ (W has mass dimension 4, while Φ has mass dimension 3/2 in 5D). For the present purpose, the important point is that the scalar background, $\phi(y) \equiv \langle \Phi(y) \rangle$, can be obtained by solving the *first order* differential equation ²

$$\phi'(y) = \frac{1}{2} \frac{\partial W(\phi)}{\partial \phi}, \quad (4)$$

and that once the solution $\phi(y)$ is found, $A'(y)$ is simply given by

$$A'(y) = \frac{1}{6M_5^3} W(\phi(y)), \quad (5)$$

which can be integrated immediately to yield $A(y)$.³ Eq. (4) shows that ϕ' is even under $y \rightarrow -y$, provided $\partial W/\partial \phi$ is even—hence $W(\phi)$ is odd—under $\phi \rightarrow -\phi$. It then follows from Eq. (5) that $A'(y)$ is odd, and therefore $A(y)$ is even under $y \rightarrow -y$, as we want. Thus, imposing the Z_2 reflection symmetry allows us to focus on odd superpotentials. We also see that for the stabilizing scalar, Φ , the discrete symmetry should be a combination of the geometric reflection $y \rightarrow -y$ and an internal parity symmetry: the action of the relevant Z_2 on the GW scalar is $\Phi(x^\mu, y) \rightarrow -\Phi(x^\mu, -y)$. The scalar potential derived from Eq. (3) is clearly even under this Z_2 , and the latter is respected by odd ‘‘kink-like’’ profiles for the VEV, $\phi(y)$.

For instance, the simplest ansatz for the superpotential is a linear one:

$$W_1(\Phi) = 2m\phi_0\Phi, \quad (6)$$

where, for later convenience, we have parameterized the coefficient in terms of a mass scale m and a scalar ‘‘VEV’’ ϕ_0 (with mass dimension 3/2). Both Eqs. (4) and (5) can be trivially integrated, and give

$$\phi(y) = \phi_0 m y, \quad (7)$$

$$A(y) = \frac{\phi_0^2 m^2}{6M_5^3} y^2, \quad (8)$$

²Eqs. (4) and (5) guarantee that the equations of motion for the gravity/scalar system are satisfied when the potential is given by Eq. (3); see [44] for details.

³Alternatively, given $A(y)$ one can combine Eqs. (4) and (5) using $\partial_\phi = (1/\phi')\partial_y$ to obtain $\phi' = \pm\sqrt{12M_5^3 A''(y)}$, which can be integrated to yield $\phi(y)$, up to a sign. If $\phi(y)$ can be inverted to obtain $y = y(\phi)$, the superpotential is given by $W(\phi) = 6M_5^3 A'(y(\phi))$.

where the condition $\phi(-y) = -\phi(y)$ sets the integration constant to zero in Eq. (7), and we choose $A(0) = 0$ by rescaling the 4D coordinates by the appropriate constant scale factor. This simple example will turn out to capture the correct physics of a large class of superpotentials, once the radion is stabilized and a hierarchy is induced.

A richer example arises from a cubic superpotential:

$$W_3(\Phi) = \frac{2m}{\phi_0} \left(\phi_0^2 \Phi - \frac{1}{3} \Phi^3 \right) , \quad (9)$$

with m an arbitrary mass scale that, without loss of generality, can be chosen to be positive. In this case, Eq. (4) reads

$$\phi'(y) = \frac{m}{\phi_0} [\phi_0^2 - \phi(y)^2] , \quad (10)$$

which can be recognized to give the standard flat space ‘‘kink’’ solution ⁴

$$\phi(y) = \phi_0 \tanh(my) , \quad (11)$$

with a thickness of order $1/m$ and asymptotic VEV $\pm\phi_0$. Following the above described procedure, one then finds

$$A(y) = \frac{\bar{k}}{4m} [\tanh^2(my) + 4 \log \cosh(my)] , \quad (12)$$

where we defined the scale \bar{k} by $\phi_0^2 = 9\bar{k}M_5^3/(2m)$, and again we chose $A(0) = 0$. Unlike the example defined by the linear superpotential (6), this model has the virtue that for $|y| \gg 1/m$ one has $A(y) \rightarrow \bar{k}|y| + \text{const.}$, so that asymptotically one gets AdS₅ with curvature given by \bar{k} . In fact, it is clear that this corresponds to the limit where the domain-wall (11) is very narrow, i.e. $m \gg \bar{k}$, and models a UV brane at $y = 0$, so that the RS solution is recovered.

We note that the potential that follows from the cubic superpotential (9) is

$$V(\Phi) = \frac{9}{4} m \bar{k} M_5^3 - m^2 \left(1 + \frac{3\bar{k}}{m} \right) \Phi^2 + \frac{4m^2}{9M_5^3} \left(1 + \frac{m}{4\bar{k}} \right) \Phi^4 - \frac{4m^3}{243\bar{k}M_5^6} \Phi^6 . \quad (13)$$

From an effective field theory perspective, this is a scalar potential subject to a parity symmetry $\Phi \rightarrow -\Phi$, and truncated at sixth order in Φ . However, it is non-generic in two ways. First, the constant term has a fixed value, which is necessary for the ansatz of Eq. (2) –with flat 4D sections– to hold. In addition to this well-known Cosmological Constant Problem, we see that the potential contains three operators that are controlled by only two parameters, thus seemingly implying an additional fine-tuned relation (at least in the absence of supersymmetry). The two parameters can be chosen as \bar{k}/M_5 and m/M_5 (M_5 simply sets the overall scale, and is associated to the strength of the gravitational interactions). However,

⁴The scalar potential, Eq. (13), depends only on ϕ_0^2 . The sign of ϕ_0 parameterizes the two solutions related by $y \rightarrow -y$, which correspond to a positive/negative VEV at $y = +\infty$.

we stress that this additional relation plays no essential role in our applications. Indeed, we see that in the thin domain-wall limit, $m \gg \bar{k}$, and using $|\phi(y)| < \phi_0$, the ratio of the Φ^6 operator to the Φ^4 operator in Eq. (13) is of order $\bar{k}/m \ll 1$. Hence, the dynamics is controlled by the quadratic and quartic operators, the last term in Eq. (13) representing only a small perturbation. In the opposite limit, $m \rightarrow 0$, and for $|\phi| \sim \phi_0$, the three operators are parametrically equally important. Nevertheless, in the central region, where $|\phi(y)| \ll \phi_0$, the dynamics is actually controlled only by the quadratic term, thus reducing precisely to the case of the linear superpotential of Eq. (6). As we will see, this will be important in the following and makes our results rather generic. The point is that we are using the special class of potentials that can be obtained from a superpotential via Eq. (3) only to obtain simple, closed solutions that fully take into account the backreaction of the scalar on the geometry, but our physical results will not depend on this simplifying assumption.

Our final example is based on the observation that the cubic superpotential above corresponds to the first two terms in the Taylor expansion of a sine:

$$W(\Phi) = \sqrt{2}m\phi_0^2 \sin\left(\sqrt{2}\frac{\Phi}{\phi_0}\right). \quad (14)$$

This leads to a scalar profile

$$\phi(y) = \sqrt{2}\phi_0 \tan^{-1}\left[\tanh\left(\frac{my}{\sqrt{2}}\right)\right], \quad (15)$$

that is also a domain wall of width of order $1/m$, centered at $y = 0$.⁵ Correspondingly,

$$A(y) = \frac{k}{\sqrt{2}m} \log\left[\cosh\left(\sqrt{2}my\right)\right], \quad (16)$$

where now ϕ_0 and k are related by $\phi_0^2 = 6kM_5^3/(\sqrt{2}m)$, and we again made sure that the warp factor is normalized to unity at $y = 0$. As in the second example, the geometry is asymptotically AdS_5 with curvature k , i.e. one has $A(y) \rightarrow k|y| + \text{const.}$ for $|y| \gg 1/m$. Again, the IR-UV-IR model of Ref. [22] arises in the limit $m \gg k$. Our comments above also apply to this example: although the potential that follows from Eq. (3) with the superpotential (14) contains an infinite tower of operators, only a few of them are actually relevant in determining the background solution: the quadratic and quartic terms in the “UV-brane” limit, $m \gg k$, and the quadratic term in the central region $y < 1/m$. Nevertheless, the “sine superpotential” has the advantage that it allows us to interpolate between narrow and wide domain-walls with a simpler warp factor than for the cubic superpotential. For concreteness, in the numerical studies of the rest of this work we will use Eqs. (15) and (16), with the understanding that the results differ from the other (and similar) examples only in minute details.

⁵The asymptotic VEV’s are $\pm(\pi/2\sqrt{2})\phi_0 \approx \pm 1.11\phi_0$.

2.2 Radion Stabilization

We described in the previous subsection the *bulk* solutions that follow from a given superpotential. However, one must ensure that these solutions are actually allowed by the boundary conditions at $y = \pm L$. One can see immediately from Eqs. (4) and (5) that this requires

$$\phi'(\pm L) = \frac{1}{2} \frac{\partial W(\phi)}{\partial \phi} \Big|_{y=\pm L}, \quad A'(\pm L) = \frac{1}{6M_5^3} W(\phi) \Big|_{y=\pm L}. \quad (17)$$

On the other hand, the set of consistent boundary conditions can be found by varying the action Eq. (1) with respect to both Φ and A , and requiring that the surface terms obtained from the integrations by parts vanish. Assuming that \mathcal{L}_4 in Eq. (1) does not involve y derivatives, e.g. if it is a pure potential term, this leads to [44]

$$\Phi'(\pm L) = -\frac{1}{2} \frac{\partial \mathcal{L}_4}{\partial \Phi} \Big|_{y=\pm L}, \quad A'(\pm L) = -\frac{1}{6M_5^3} \mathcal{L}_4 \Big|_{y=\pm L}. \quad (18)$$

Following Refs. [44, 16] one can enforce that the scalar field attain a given value $\bar{\phi}_0$ (in absolute magnitude) at the boundaries by writing an even boundary term ⁶

$$\Delta \mathcal{L}_4(\Phi) = -\gamma (\Phi^2 - \bar{\phi}_0^2)^2, \quad (19)$$

that does not contribute to Eqs. (18) in the limit $\gamma \rightarrow +\infty$. Thus, we see that one can use

$$\mathcal{L}_4(\Phi) = -W(\bar{\phi}_0) - W'(\bar{\phi}_0)(\Phi - \bar{\phi}_0) + \Delta \mathcal{L}_4(\Phi), \quad (20)$$

which leads to Eqs. (17) [for $\gamma \rightarrow +\infty$], as required. In the limit of a fixed VEV, $\bar{\phi}_0$, at the boundaries, we must have

$$\bar{\phi}_0 = \phi(L) = \sqrt{2}\phi_0 \tan^{-1} \left[\tanh \left(\frac{mL}{\sqrt{2}} \right) \right], \quad (21)$$

where the second equality holds for the case of the ‘‘sine’’ superpotential, Eq. (14). This equation fixes the size of the extra dimension to be

$$mL = \sqrt{2} \tanh^{-1} \left[\tan \left(\frac{\bar{\phi}_0}{\sqrt{2}\phi_0} \right) \right], \quad (22)$$

and depends only on the ratio $\bar{\phi}_0/\phi_0$. ⁷ Then Eq. (16) gives

$$A(L) = \frac{k}{\sqrt{2}m} \log \left[\cosh \left(\sqrt{2}mL \right) \right], \quad (23)$$

⁶One can also write $\Delta \mathcal{L}_4 = -\gamma (\Phi - \bar{\phi}_0)^2$ at $y = +L$, and $\Delta \mathcal{L}_4 = -\gamma (\Phi + \bar{\phi}_0)^2$ at $y = -L$, so as to preserve the $\Phi(y) \rightarrow -\Phi(-y)$ symmetry. In this case, the constant γ has positive mass dimension and perhaps it is more natural than in the case of Eq. (19) for it to take a large value. It also has the virtue that it selects the ‘‘domain-wall scalar profile’’ over a constant profile. In any case, the most important (simplifying) assumption is that the value of the scalar field be frozen on the boundaries.

⁷Notice that if $\bar{\phi}_0/\phi_0$ is such that $|\tan(\frac{\bar{\phi}_0}{\sqrt{2}\phi_0})| > 1$ there are no (real) solutions for L from Eq. (22). This is simply the statement that the brane VEV, $\bar{\phi}_0$, cannot be larger than the asymptotic VEV of the bulk solution, Eq. (15), for the configuration to be allowed.

which is parametrically large for $m \ll k$, i.e. away from the “thin UV brane” limit, even when $mL \sim \mathcal{O}(1)$. It is also large in the limit that the extra dimension is large, $mL \gg 1$ and $kL \gg 1$, although this requires the brane and bulk VEV’s to satisfy $\bar{\phi}_0/(\sqrt{2}\phi_0) \approx \pi/4$, a tuned limit.

2.3 From Large to Small Warping

The model described above depends on three dimensionless ratios: k/m , $\bar{\phi}_0/\phi_0$ and k/M_5 . The latter ratio determines the degree of warping (from nearly flat when $k \ll M_5$, to strongly warped when $k \sim M_5$). The case of small warping may require fine-tuning to make the 5D cosmological constant much smaller than the fundamental scale M_5 (in addition to the fine-tuning associated with the vanishing of the 4D CC). Nevertheless, we will consider such a small warping limit since it allows us to make the connection with the well-studied models of Universal Extra Dimensions (UED) [24], which assume that the 5D curvature is negligible, while still showing some interesting differences when k is small but non-vanishing. In the opposite limit of strong warping we can place a rough upper bound on the size of the curvature from the requirement that there be some modest hierarchy between k and the cutoff of the theory, Λ_5 , so that neglecting higher-dimension operators in the Einstein-Hilbert action is justified. Based on NDA in extra-dimensional theories [45] we expect that $\Lambda_5^3 \sim M_5^3/l_5$, with $l_5 = 24\pi^3$, a 5D loop factor. This suggests that even for $k = M_5$, one has $\Lambda_5 \sim 10k$, which is a large enough separation for the 5D EFT to be useful. Hence, whenever we need to be concrete, we will take $k = M_5$ when discussing the strong warping limit, although cases where k is somewhat smaller can be considered.

We can further constrain the parameter space based on phenomenological considerations. First, one must reproduce the 4D Planck scale, $M_P \approx 2.4 \times 10^{18}$ GeV. Second, as will be seen in the following sections, the scale of KK resonances is set by $\tilde{k} \equiv k e^{-A(L)}$.⁸ We will assume that $\tilde{k} \sim \mathcal{O}(1 \text{ TeV})$ to open the window to test this scenarios at the LHC. These two constraints determine M_5 and one of the three dimensionless parameters mentioned above. One can exchange one of the two remaining parameters for the radion decay constant Λ_r (to be discussed in Section 3.1), plus a free dimensionless parameter that we will choose as k/m . We elaborate next on the first two relations, before discussing the properties of the radion field.

2.3.1 The 4D Planck Scale

We start by computing the effective 4D Planck scale from the underlying Lagrangian parameters. For instance, in the model defined by Eq. (14) the 4D (reduced) Planck mass is

$$M_P^2 = M_5^3 \int_{-L}^L e^{-2A(y)} dy = \frac{2M_5^3}{m} \int_0^{mL} dx \left[\cosh(\sqrt{2}x) \right]^{-\sqrt{2}k/m}, \quad (24)$$

⁸To be more precise, the KK scale is set by the warped down curvature scale at the IR boundaries, $k_{\text{eff}} e^{-A(L)}$, where $k_{\text{eff}} = A'(L) = s_A k$, and s_A is a model-dependent number smaller than one. See Eq. (28) below.

where the factor of 2 arises from the Z_2 symmetry of the background about $y = 0$. There are three important scales in the problem: the curvature k , the width of the domain wall $1/m$, and the size of the extra dimension L . As will be shown in the next subsection, we will be most interested in the case where $m \ll k$, i.e. when the domain wall is thick in units of the curvature scale. In this case, we find that M_P^2 is well approximated by

$$M_P^2 \approx \frac{2M_5^3}{m} \times \sqrt{\frac{\pi m}{4\sqrt{2}k}} \tanh\left(\sqrt{\frac{2k}{m}} \times mL\right). \quad (25)$$

From this expression we see that unless the extra dimension is so small that $mL \ll \sqrt{m/k}$, the tanh is essentially equal to one and we have $M_P^2 \approx (\pi/\sqrt{2})^{1/2} M_5^3/\sqrt{km} \approx 1.49M_5^3/\sqrt{km}$.

For completeness, we also give an approximate expression that holds in the narrow domain wall approximation, $m \gg k$:

$$\begin{aligned} M_P^2 &= \frac{2M_5^3}{k} \int_0^{kL} dz \left[\cosh\left(\frac{m}{k}\sqrt{2}z\right) \right]^{-\sqrt{2}k/m} \\ &\approx \frac{2M_5^3}{k} \left[2^{\sqrt{2}k/m-1} \left(e^{-\sqrt{2}k/m} - e^{-2kL} \right) + \frac{k}{\sqrt{2}m} \right]. \end{aligned} \quad (26)$$

In the limit that $k/m \rightarrow 0$ we recover the RS result $M_P^2 = (1 - e^{-2kL}) M_5^3/k$ [1].

2.3.2 Constraints from TeV Scale New Physics

We now explain how to further constrain the model parameters. Imposing that the observed M_P be reproduced, and for given k/M_5 , Eq. (24) determines k as a function of k/m and mL . Fixing also $\tilde{k} \equiv k e^{-A(L)}$, one finds the “required” warp factor from $A(L) = \ln k/\tilde{k}$. Comparing to Eq. (23) allows one to fix mL , for given k/m .⁹ One can then find $\bar{\phi}_0/\phi_0$ from Eq (22).

At this point the model is determined by $\epsilon \equiv k/M_5$ and k/m . In the left panel of Fig. 1, we show lines of constant mL in the $\epsilon - (k/m)$ plane, requiring that $M_P = 2.4 \times 10^{18}$ GeV and $\tilde{k} = 1$ TeV. This shows how to reach the regions of small ($k \ll M_5$) and large ($k \lesssim M_5$) warping. In the right panel, we show what this implies for the ratio M_5/M_P (recall that M_5 is regarded as the fundamental scale in the theory, while M_P appears as an effective scale characterizing the interactions of the zero-mode graviton).

Of course, naturality considerations lead to the expectation that k and M_5 should not be very different, and that $k \sim M_5 \sim M_P$ as in the Randall-Sundrum proposal. In Fig. 2 we plot $A(L)$ and mL as a function of k/m , assuming that $M_5 = k$. We see that $A(L)$ remains essentially constant at $A(L) \sim 34-35$. The curvature scale varies between $(0.5 - 1.4) \times 10^{18}$ GeV in the shown range. At the same time $\bar{\phi}_0/\phi_0$ varies from $\bar{\phi}_0/\phi_0 \sim 1.1$ for $k/m \sim \text{few}$,

⁹For $m \ll k$, Eq. (25) shows that M_P becomes essentially independent of mL once $mL > \sqrt{m/k}$, while for $m \gg k$ Eq. (26) shows that M_P becomes essentially independent of mL for $mL > m/k$; in either of these limits fitting M_P effectively determines k as a function of k/m . Then mL is fixed as a function of k/m from Eq. (23).

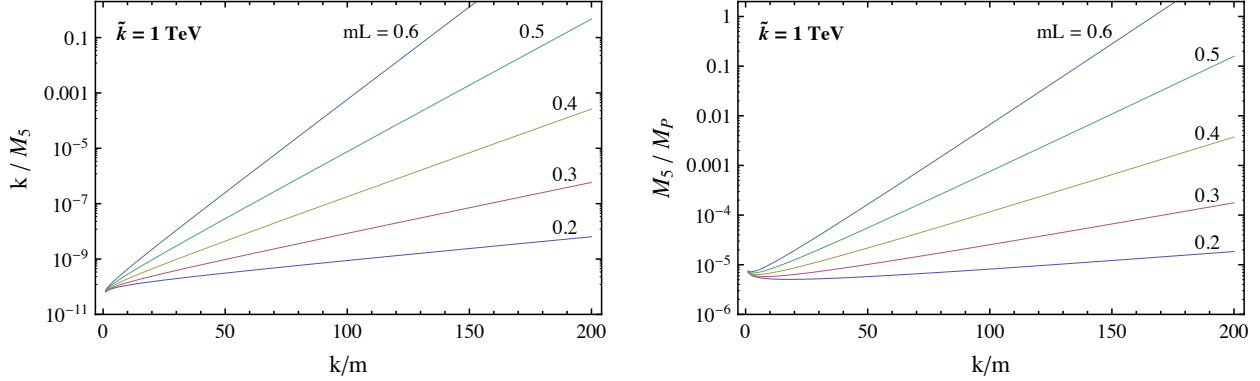


Figure 1: k/M_5 (left panel) and M_5/M_P (right panel) as a function of k/m for different values of mL , and for fixed $\tilde{k} \equiv k e^{-A(L)} = 1$ TeV.

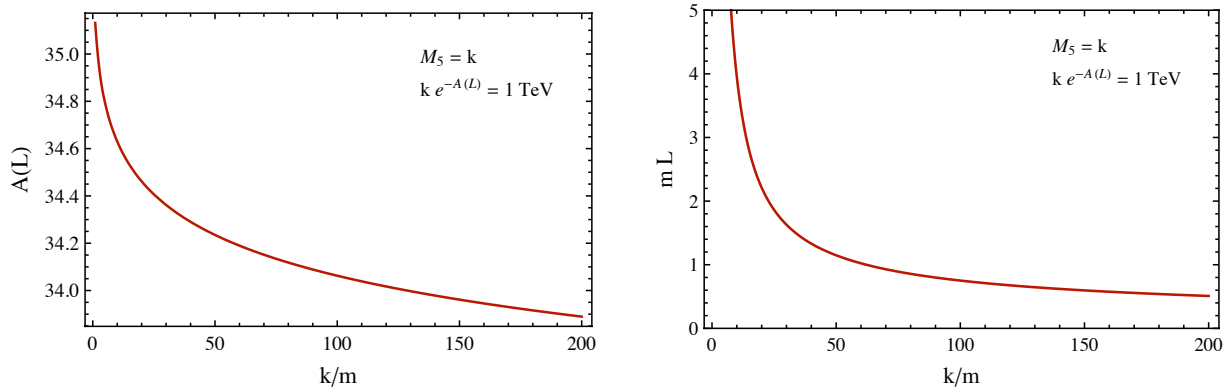


Figure 2: $A(L)$ from Eq. (23) (left panel), and mL from Eq. (22) (right panel) as a function of k/m . We impose Eq. (24) assuming $M_5 = k$ and $\tilde{k} \equiv k e^{-A(L)} = 1$ TeV.

down to $\bar{\phi}_0/\phi_0 \sim 0.5$ for $k/m \sim 200$. The right panel of Fig. 2 shows that $mL \gtrsim 1$ (we also point out that $35 \lesssim kL \lesssim 100$ in the range shown in the figures). However, large values of mL require $\bar{\phi}_0/(\sqrt{2}\phi_0) \approx \pi/4$, so that in general we expect $mL \sim \mathcal{O}(1)$, and therefore we need $k/m \gg 1$ to generate the hierarchy. This means that the physical space is expected to be restricted to the “central region” of the domain-wall solution. As discussed in the previous subsection, in this region the background solution is dominated by the quadratic term in the scalar potential, and can be simply modeled by the linear superpotential of Eq. (6).

The small warping regime can be obtained for any value of k/m with $mL \lesssim 1$, as seen in the left panel of Fig. 1. For $k/m \sim 1$, Eq. (23) implies that $A(L) \sim \mathcal{O}(1)$, so that there is virtually no warping. In this case, the Planck-weak scale hierarchy is directly set by $\tilde{k}/M_P \sim (k/M_5) \times (M_5/M_P) \sim 10^{-15}$, as can be seen from Fig. 1.¹⁰ For $k/m \gg 1$ one

¹⁰Note that this gives a scenario qualitatively similar to the UED models, where $1/L \sim k \sim \tilde{k} \sim \text{TeV}$, but $M_5 \sim 10^{13}$ GeV. Since the couplings among KK modes are of the same order as those of the 0-modes (recall $A(L) \sim 1$), the 4D EFT breaks down at $\mathcal{O}(100) \times k$, as in UEDs. However, as in warped scenarios, one would expect that UV brane observables are under control up to scales of order M_5 .

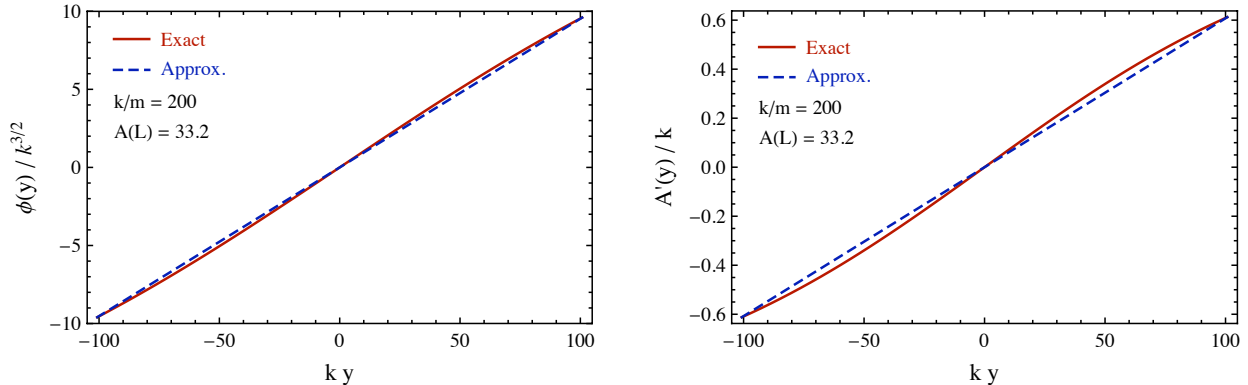


Figure 3: *Left panel:* $\phi(y)$ in units of $k^{3/2}$ for the “sine” superpotential (solid, red line), and the approximation of Eq. (27) (dashed, blue line). *Right panel:* $A'(y)$ in units of k for the “sine” superpotential (solid, red line), and the approximation of Eq. (28) (dashed, blue line).

arrives at the interesting situation where the Planck-weak scale hierarchy arises in part from a sizable warping $1 < A(L) \ll \mathcal{O}(35)$ as well as from a hierarchy associated with a small curvature $k \ll M_5$.

2.3.3 The Limit of a Fat UV Brane: Benchmark Scenarios

The previous considerations suggest that we focus on the regime $k/m \gg 1$, corresponding to a “fat UV brane”. In this case, $\phi(y)$ and $A(y)$ can be approximated by linear and quadratic functions of y as follows:

$$\phi(y)/\phi_0 \approx s_\phi y/L, \quad (27)$$

$$A(y) \approx s_A k y^2 / (2L), \quad (28)$$

where $s_\phi = \sqrt{2} \tan^{-1} \left[\tanh \left(\frac{mL}{\sqrt{2}} \right) \right]$ and $s_A = \tanh(\sqrt{2}mL)$ in the model defined by the “sine” superpotential, Eq. (14). In other models, s_ϕ and s_A will have a different dependence on the microscopic parameters, but will still be numbers of order one, so that Eqs. (27) and (28) provide a general parameterization of “fat brane scenarios”, which we will call “the linear regime”. The accuracy of the linear regime for $k/m \gg 1$ can be seen in Fig. 3, where we plot $\phi(y)$ and $A'(y)$ as a function of ky , for the exact expressions (15) and (16), as well as for the approximations (27) and (28). In the following we will make extensive use of the approximate expressions (27) and (28) to gain intuition (and relatively accurate simple expressions) for the spectrum and couplings of KK modes.

Here we will summarize the parameters for two “benchmark scenarios” that we will use in some of the numerical studies that follow. Both are based on the “sine” superpotential, i.e. on the profiles of Eqs. (15) and (16). As we will see in the following, $k_{\text{eff}} \equiv A'(L) (= s_A k)$ plays an important role.

- “*Strong warping scenario*”: we take $M_5 = k$, $\tilde{k} = 2$ TeV and $k/m = 200$, apart from the phenomenological constraints discussed above. In this case, one finds $k \approx$

5.2×10^{17} GeV, $A(L) \approx 33.2$, $mL \approx 0.50$, $k_{\text{eff}}L \approx 62$, $\bar{\phi}_0/\phi_0 \approx 0.47$. For reference, the radion decay constant, to be defined in the next section, is $\Lambda_r = 4.4$ TeV.

- “*Small warping scenario*”: we take $M_5 = 2 \times 10^8 k$, $\tilde{k} = 2$ TeV and $k/m = 200$, apart from the phenomenological constraints discussed above. In this case, one finds $k \approx 1.8 \times 10^5$ GeV, $A(L) \approx 4.5$, $mL \approx 0.18$, $k_{\text{eff}}L \approx 9$, $\bar{\phi}_0/\phi_0 \approx 0.18$. The radion decay constant is $\Lambda_r = 2 \times 10^{16}$ GeV. This example lies approximately at the right end of the blue, lower curve of Fig. 1.

Here we have taken a relatively large value for $k/m = 200$. This is only to make sure that we are in the linear approximation of Eqs. (27) and (28), since some of the simple analytic expressions to be derived in the following sections rely on being in the linear regime. However, it is possible to take a smaller hierarchy between k and m , and we provide formulas for the general case as well. We also point out that the most notable difference between the strong and small warping scenarios enters through the radion decay constant, Λ_r , and is therefore relevant for radion or KK-radion phenomenology. The specific “small” warping scenario is inspired by a scenario for KK-radion dark matter, to be presented in [29].

We should also add that there are further phenomenological constraints on the KK scale from EW precision tests, and possibly from flavor and CP violating observables. However, such bounds depend on the particular model under consideration. Given that our emphasis in this paper is on the general framework, we do not engage in the detailed study of such constraints. Nevertheless, we have chosen our “strong warping scenario” in such a way that the KK gluon mass, $M_{\text{KK}} \approx 2.39 \tilde{k}_{\text{eff}} \sim 3$ TeV (see caption to Table 1 at the end of this paper), is roughly consistent with the bounds studied in other warped scenarios. For the “small warping scenario” we allow a smaller $M_{\text{KK}} \approx 2.19 \tilde{k}_{\text{eff}} \sim 1$ TeV (see caption to Table 2) since we expect the bounds to be somewhat looser in that case (somewhat similar to the UED case). We stress, however, that the data we present in this work are largely independent of the precise value of M_{KK} , within a given gravitational background, and should be useful when more detailed studies of the bounds on the KK scale in given models are performed.

3 Properties of the Radion KK Tower

We now turn to the scalar excitations associated with the background described in the previous section, paying special attention to the lightest KK-parity even scalar (the “radion”) and the lightest KK-parity odd scalar (that will turn out to be the LKP).

3.1 Normalization and Radion Decay Constant

We start by discussing the normalization of the radion/scalar KK modes in general. Following Ref. [16] we parameterize the 4D physical scalar fluctuations (after gauge fixing) in the 5D metric/bulk scalar system by

$$ds^2 = e^{-2A(y)-2F(x,y)} \eta_{\mu\nu} dx^\mu dx^\nu - [1 + 2F(x, y)]^2 dy^2, \quad (29)$$

$$\Phi(x, y) = \phi(y) + \varphi(x, y) , \quad (30)$$

where $A(y)$ and $\phi(y)$ are the background profiles described in the previous section, and

$$\varphi(x, y) = \frac{3M_5^3}{\phi'(y)} e^{2A(y)} \partial_y [e^{-2A(y)} F(x, y)] . \quad (31)$$

In terms of the KK decomposition

$$F(x, y) = \sum_{n=0}^{\infty} \tilde{r}_n(x) F_n(y) , \quad (32)$$

one can show [16] that $F_n(y)$ obeys the ‘‘KK radion-scalar’’ equation of motion ¹¹

$$F_n'' - 2A'F_n' - 4A''F_n - 2\frac{\phi''}{\phi'}F_n' + 4A'\frac{\phi''}{\phi'}F_n + e^{2A}m_n^2F_n = 0 , \quad (33)$$

with boundary condition (in the limit that the Φ VEV is frozen at the boundaries)

$$(F_n' - 2A'F_n)|_{\pm L} = 0 , \quad (34)$$

guaranteeing the self-adjointness of Eq. (33). In order to see the orthogonality relations for the KK wavefunctions that follow from this, it is useful to remove the terms proportional to F_n' in Eq. (33) by defining $\hat{F}_n(y) = e^{-A(y)} F_n(y) / \phi'(y)$ so that:

$$\hat{F}_n'' - \left[A'^2 + 3A'' - 2A' \frac{\phi''}{\phi'} + 2 \frac{\phi''^2}{\phi'^2} - \frac{\phi'''}{\phi'} - e^{2A} m_n^2 \right] \hat{F}_n = 0 . \quad (35)$$

The standard argument then leads to the orthogonality condition, $\int_{-L}^L dy e^{2A} \hat{F}_m \hat{F}_n \propto \delta_{mn}$. If we use the relation $\phi'^2 = 3M_5^3 A''$, implied by the Einstein equations for the background, we get the orthonormality relation for $F_n(y)$:

$$\int_{-L}^L dy \frac{F_m(y) F_n(y)}{A''(y)} = \frac{e^{-2A(L)}}{k_{\text{eff}} m_n^2} \delta_{mn} , \quad (36)$$

where the normalization of the wavefunctions, including the presence of the KK radion masses m_n , was chosen for later convenience.

Replacing Eqs. (29)-(31) and the KK decomposition of Eq. (32) in the action of Eq. (1), one finds that the Einstein-Hilbert term results in a contribution to the kinetic terms of the radion KK-modes, \tilde{r}_n , given by $3M_5^2 \int d^5x e^{-2A} F_m F_n \partial_\mu \tilde{r}_m \partial^\mu \tilde{r}_n$, where the derivatives are contracted with the Minkowski metric. Similarly, the scalar part of the action gives a contribution to the KK radion kinetic terms of $\int d^5x \frac{1}{2} e^{-2A} f_n f_m \partial_\mu \tilde{r}_m \partial^\mu \tilde{r}_n$, with $f_n =$

¹¹Sometimes it is useful to write this equation as $\phi'^2 \partial_y \left\{ \frac{e^{2A}}{\phi'^2} \partial_y [e^{-2A} F_n] \right\} + (e^{2A} m_n^2 - 2A'') F_n = 0$, which suggests the relation between the existence of a massless radion mode, with $F_0 \propto e^{2A}$, and $A'' = 0$.

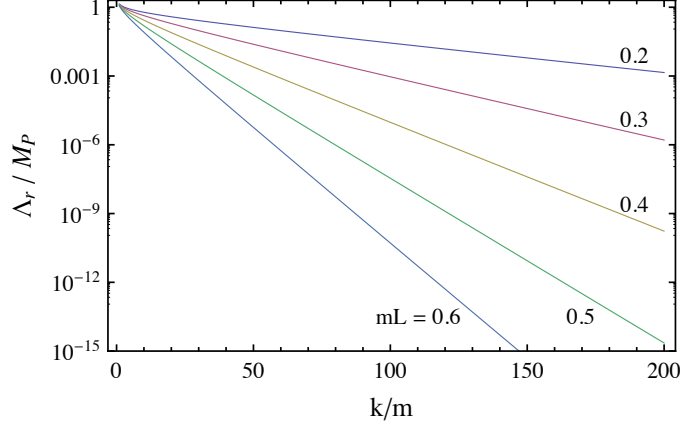


Figure 4: Λ_r/M_P as a function of k/m for several values of mL . Recall that $M_P = 2.4 \times 10^{18}$ GeV is the reduced Planck mass.

$\frac{3M_5^3}{\phi'} e^{2A} \partial_y (e^{-2A} F_n)$. After integration by parts with respect to y , and using the KK radion equation (33) together with the relation $\phi'^2 = 3M_5^3 A''$, this generates a term that precisely cancels the Einstein-Hilbert contribution, leaving behind only the terms proportional to m_n^2 . The action Eq. (1) at quadratic order in $\tilde{r}_n(x)$ then reads:

$$\begin{aligned}
 S &= \frac{3}{2} M_5^3 \sum_{m,n} \int d^4x m_n^2 \int_{-L}^L dy \frac{F_m(y) F_n(y)}{A''(y)} \partial_\mu \tilde{r}_m \partial^\mu \tilde{r}_n + \dots, \\
 &= \Lambda_r^2 \int d^4x \sum_n \frac{1}{2} \partial_\mu \tilde{r}_n(x) \partial^\mu \tilde{r}_n(x) + \dots,
 \end{aligned} \tag{37}$$

where we used the orthonormality relation (36), while the dots stand for higher order or non-derivative terms, and contain the potential for \tilde{r}_n . We also defined the radion decay constant

$$\Lambda_r = \sqrt{\frac{3M_5^3}{k_{\text{eff}}}} e^{-A(L)}. \tag{38}$$

In the case that Eq. (25) holds, i.e. for $m \ll k$, we have $\Lambda_r \approx (2/s_A)^{1/2} \left(\frac{m}{k}\right)^{1/4} M_P e^{-A(L)}$. As remarked in Section 2.3, the hierarchy between k and M_5 affects mostly the value of Λ_r , for fixed $\tilde{k} = k e^{-A(L)}$. As $\epsilon = k/M_5$ decreases, Λ_r increases, while for $k \sim M_5$, one has $\Lambda_r \sim \tilde{k}$. Thus, we see that the couplings of the radion are very sensitive to the size of the 5D curvature. In Fig. 4, we show Λ_r/M_P as a function of k/m for several values of mL , in the ‘‘sine’’ model of Eqs. (22) and (23). This plot should be compared to Fig. 1, but it is important to note that Λ_r/M_P is actually independent of \tilde{k} .

3.2 Radion Mode

In this subsection, we study the lightest excitations of Eq. (33). Since in the limit that $A''(y) = 0$ there is a zero-mode solution with wavefunction $F_0 \propto e^{2A}$, it is convenient to write in the general case

$$F_0(y) \propto e^{2A(y)+g(y)} , \quad (39)$$

so that the radion equation of motion and the boundary conditions reduce to

$$g'' + g'^2 + 2 \left(A' - \frac{\phi''}{\phi'} \right) g' = 2A'' - e^{2A} m_0^2 , \quad (40)$$

$$g'|_{\pm L} = 0 . \quad (41)$$

Note that the differential equation is of first order in g' . We can obtain a good approximation to the ultralight mode with mass m_0 by neglecting the g'^2 term, in which case Eq. (40) is solved by

$$g'(y) = e^{-2A(y)} \phi'(y)^2 \left[2 \int_0^y dz \frac{A''}{\phi'^2} e^{2A} - m_0^2 \int_0^y dz \frac{e^{4A}}{\phi'^2} \right] , \quad (42)$$

where we chose the constant of integration so that $g'(0) = 0$ (since the radion is even about $y = 0$). The boundary condition (41) then implies

$$m_0 = \sqrt{\frac{2 \int_0^L dz \frac{A''(z)}{k_{\text{eff}}^2 \phi'(z)^2} e^{2A(z)}}{\int_0^L \frac{dz}{\phi'(z)^2} e^{4A(z)-2A(L)}}} k_{\text{eff}} e^{-A(L)} , \quad (43)$$

which is a rather general expression for the ‘‘radion’’ mass in terms of $\phi(y)$ and $A(y)$. Here we have expressed the result in terms of $k_{\text{eff}} = A'(L) = s_A k$.

For instance, for the ‘‘strong’’ (‘‘small’’) warping benchmark scenarios defined at the end of Subsection 2.3.3, we obtain from Eq. (43) that $m_0 = 0.22 \tilde{k}_{\text{eff}}$ ($m_0 = 0.67 \tilde{k}_{\text{eff}}$), which agrees very well with the numerical solution obtained without any approximations (here $\tilde{k}_{\text{eff}} \equiv k_{\text{eff}} e^{-A(L)}$). The neglected g'^2 term contributes negligibly to the mass because it is comparable to the other terms in Eq. (40) only for y 's near the UV brane, but the wavefunction profile, Eq. (39), is exponentially localized near the boundaries at $y = \pm L$. Hence distortions near the UV region can only give an exponentially small effect.

As explained in Section 2, in order to solve the Planck/weak scale hierarchy problem the size of the fifth dimension is often stabilized in a region where $\phi(y)$ and $A(y)$ are well approximated by linear and quadratic functions in y , as given in Eqs. (27) and (28), respectively. Note that the radion EOM, Eq. (33), is approximately independent of the scalar profile, since $\phi'' \approx 0$ in this limit. In this case, we can write a simpler expression for m_0 that is independent of the scalar profile:

$$m_0 \approx \sqrt{\frac{2}{k_{\text{eff}} L} \frac{\int_0^L dz e^{2A(z)}}{\int_0^L dz e^{4A(z)-2A(L)}}} k_{\text{eff}} e^{-A(L)} \quad (44)$$

$$\approx \frac{2}{\sqrt{k_{\text{eff}}L}} k_{\text{eff}} e^{-A(L)} , \quad (45)$$

where in the second line we used that when $A(y)$ is given by Eq. (28), the ratio of integrals in Eq. (44) is very close to 2.¹² For the “strong” (“small”) warping benchmark scenarios of Subsection 2.3.3, Eq. (44) gives $m_0 = 0.26 \tilde{k}_{\text{eff}}$ ($m_0 = 0.68 \tilde{k}_{\text{eff}}$), while Eq. (45) gives $m_0 \approx 0.25 \tilde{k}_{\text{eff}}$ ($m_0 \approx 0.67 \tilde{k}_{\text{eff}}$).

For future reference, we also give an approximate expression for the radion wavefunction, normalized according to Eq. (36), in the limit that $A(y)$ is well approximated by Eq. (28). The fact that the radion mass is parametrically smaller than the KK scale, \tilde{k}_{eff} , corresponds to the fact that $g(y)$ in Eq. (39) is a small perturbation. Therefore, setting $g(y) \approx 0$, and using Eq. (45) for m_0 , we obtain

$$F_0(y) \approx e^{2[A(y)-A(L)]} , \quad (46)$$

where we used $\int_0^z dp e^{p^2} \approx \frac{1}{2z} e^{z^2}$, which holds whenever $z \gg 1$.

3.3 Lightest Odd-Scalar

As already mentioned, the radion profile, Eqs. (39) or (46), is exponentially localized near the boundaries at $y = \pm L$. Thus, after normalization, its value at $y = 0$ is exponentially small (while –being even– its derivative vanishes at the origin). One can then see that by adjusting m_0 by an exponentially small amount one can obtain a solution that vanishes at the origin, and therefore that there is an odd mode with a mass exponentially close to the radion mass given in Eq. (43). We can make the argument more concrete by writing $F_{\text{odd}}(y) = F(y) + \epsilon(y)$, where $F(y)$ is the radion wavefunction given in Eq. (39). Writing also $m_{n=1}^2 = m_0^2 + \delta m^2$, where m_0 is the radion mass given above, Eq. (33) becomes

$$\epsilon'' - 2\epsilon' \left(A' + \frac{\phi''}{\phi'} \right) + \epsilon \left[e^{2A} (m_0^2 + \delta m^2) - 4A'' + 4A' \frac{\phi''}{\phi'} \right] + e^{2A} \delta m^2 F = 0 . \quad (47)$$

We can approximately solve this equation in the limit where $\phi(y)$ and $A(y)$ are given by Eqs. (27) and (28), respectively, which corresponds to the limit we are interested in. In this case, the terms proportional to ϕ'' vanish. In addition, using the approximate expression for m_0 given in Eq. (45) we see that $m_0^2 e^{2A}/(4A'') \sim e^{-2[A(L)-A(y)]}$, which is much smaller than one except for $y \approx L$. Since, as we will see, also $\delta m^2 \ll m_0^2$, we can focus on solving

$$\epsilon'' - 2A'\epsilon' - 4A''\epsilon + e^{2A}\delta m^2 F \approx 0 , \quad (48)$$

with A given by Eq. (28). Its solution takes the somewhat cumbersome form

$$\epsilon(y) \approx e^{2A(y)} \delta m^2 \left\{ y \int_y^L dz_2 F(z_2) \left[1 - 2e^{2A(z_2)} A'(z_2) \int_{z_2}^L dz_1 e^{-2A(z_1)} \right] \right\}$$

¹²If the linear approximation is not excellent, one can obtain a pretty good approximation to the radion mass by using $m_0 \approx \sqrt{\frac{2}{k_{\text{eff}}L}} k_{\text{eff}} e^{-A(L)}$, which only assumes that, due to the strong localization of the inverse warp factor near $y = L$ over a distance of order $1/k_{\text{eff}}$, the ratio of integrals in Eq. (44) is of order one.

$$- \left[e^{-2A(y)} - 2A'(y) \int_y^L dz e^{-2A(z)} \right] \int_y^L dz z e^{2A(z)} F(z) \Big\} , \quad (49)$$

where we imposed $\epsilon(L) = \epsilon'(L) = 0$. The first condition can be obtained by requiring that $F_{\text{odd}}(L) = F(L)$ by a simple overall rescaling of the odd wavefunction, and the second follows from Eq. (34), together with the fact that the radion wavefunction, $F(y)$, already satisfies this boundary condition. We emphasize that Eq. (49) assumes that $A(y)$ is given by Eq. (28). Requiring that $F_{\text{odd}}(0) = F(0) + \epsilon(0) = 0$ fixes δm^2 as

$$\delta m^2 \approx \left\{ \int_0^L dz z k_{\text{eff}}^2 e^{2[A(z)-A(L)]} \frac{F(z)}{F(0)} \right\}^{-1} k_{\text{eff}}^2 e^{-2A(L)} \quad (50)$$

$$\approx \frac{1}{k_{\text{eff}} L} \frac{F(0)}{F(L)} k_{\text{eff}}^2 e^{-2A(L)} , \quad (51)$$

where we used $A(0) = A'(0) = 0$ to write Eq. (50), while Eq. (51) holds due to the strong localization of the radion wavefunction and the inverse warp factor near $y = L$ over a distance of order $1/k_{\text{eff}}$. This expression shows that $\delta m^2/m_0^2$ is (exponentially) small due to the IR localization of the radion wavefunction, $F(y)$. Hence, the radion and the lightest odd-scalar are exponentially degenerate in this scenario.

4 Fermions

We analyze now the fermionic sector. The Hermitian fermion action is

$$S_{\text{fermion}} = \int d^5x \sqrt{g} \left\{ \frac{i}{2} \bar{\Psi} e_A^M \Gamma^A D_M \Psi - \frac{i}{2} (D_M \Psi)^\dagger \Gamma^0 e_A^M \Gamma^A \Psi - y_\Psi \Phi \bar{\Psi} \Psi \right\} , \quad (52)$$

where $\Gamma^A = (\gamma^\mu, -i\gamma_5)$ are the flat space Dirac gamma matrices in 5D space, e_A^M is the fünfbein, D_M is the covariant derivative with respect to the gauge symmetry as well as general coordinate and local Lorentz transformations¹³, and y_Ψ is a Yukawa coupling (with mass dimension $-1/2$). In the scalar background $\langle \phi \rangle$ given in Eq. (15) the Yukawa interaction gives rise to a y -dependent mass term for the fermion, $m_D \equiv y_\Psi \langle \Phi \rangle$.

Note that the Yukawa interaction above is consistent with the Z_2 transformation $\Phi(y) \rightarrow -\Phi(-y)$ provided either $\Psi_L(y) \rightarrow \Psi_L(-y)$ and $\Psi_R(y) \rightarrow -\Psi_R(-y)$ or viceversa. This matches with the fact that, at a given KK level, the $y \rightarrow -y$ transformation properties of the wavefunctions $f_L^n(y)$ and $f_R^n(y)$ are opposite, but the associated 4D fields are nevertheless assigned the same KK parity (even for even n and odd for odd n , independent of chirality).

¹³For a diagonal metric of the form $ds^2 = a(y)^2 \eta_{\mu\nu} dx^\mu dx^\nu - b(y)^2 dy^2$ the spin connection in D_M cancels out in the fermion action, Eq. (52).

4.1 Equations of Motion and Kaluza-Klein Decomposition

Considering the action to quadratic order in the fields, the KK decomposition for each 4D chirality of the 5D fermion reads ¹⁴

$$\Psi_{L,R}(x, y) = \frac{e^{\frac{3}{2}A(y)}}{\sqrt{2L}} \sum_{n=0}^{\infty} \psi_{L,R}^n(x) f_{L,R}^n(y) , \quad (53)$$

where the fermion profiles obey the orthonormality conditions

$$\frac{1}{2L} \int_{-L}^L dy f_{L,R}^n(y) f_{L,R}^m(y) = \delta_{nm} , \quad (54)$$

and the first order equations

$$\left(\partial_y + m_D - \frac{1}{2}A' \right) f_L^n = m_n e^A f_R^n , \quad (55)$$

$$\left(\partial_y - m_D - \frac{1}{2}A' \right) f_R^n = -m_n e^A f_L^n . \quad (56)$$

The boundary conditions at $y = -L$ and $y = L$ are given either by

$$f_L^{n'} + \left(m_D - \frac{1}{2}A' \right) f_L^n \Big|_{y=\mp L} = 0 , \quad f_R^n(\mp L) = 0 , \quad (57)$$

or

$$f_R^{n'} - \left(m_D + \frac{1}{2}A' \right) f_R^n \Big|_{y=\mp L} = 0 , \quad f_L^n(\mp L) = 0 , \quad (58)$$

where $' = \partial_y$. These give rise to a chiral zero-mode sector: Eq. (57) selects a left-handed (LH) zero-mode while Eq. (58) allows only a right-handed (RH) one. The zero-mode solutions are explicitly given by

$$f_{L,R}^0(y) = N \exp \left(\frac{1}{2}A(y) \mp \int_0^y dz m_D(z) \right) , \quad (59)$$

where N is determined by Eq. (54). These solutions are even about $y = 0$ since $A(y)$ is even and the integral of the odd function $m_D(z)$ is also even.

We note that when $m_D(y)$ and $A'(y)$ are proportional to each other, which is the case when $\phi(y)$ and $A(y)$ are approximately given by Eqs. (27) and (28), the fermion zero-mode wavefunctions further simplify. In this case, we define a dimensionless parameter c by

$$m_D(y) = \pm c A'(y) , \quad (60)$$

¹⁴We use the convention that $\gamma_5 \Psi_{L,R} = \mp \Psi_{L,R}$.

where we take the upper (lower) sign when the 5D fermion has a LH (RH) zero mode (i.e. when the boundary conditions (57) or (58) hold, respectively). In our case, we have the explicit relation

$$c = \pm y_\Psi (s_\phi/s_A) (\phi_0/k) , \quad (61)$$

where s_ϕ and s_A were defined in Eqs. (27) and (28). In the limit that the proportionality of Eq. (60) holds, the zero-mode profiles of Eq. (59) take the simple form

$$f^0(y) = N_0 e^{-(c-\frac{1}{2})A(y)} , \quad (62)$$

independently of the chirality of the zero-mode sector. This shows that for $c \approx 1/2$ the zero-mode profiles are (approximately) flat, while for $c \gtrsim 1/2$ ($c \lesssim 1/2$) they are localized near the UV brane (IR boundaries). Even in cases where Eq. (60) does not hold exactly, it is useful to formally exchange the Yukawa coupling y_Ψ for a c -parameter, defined by Eq. (61), and we shall do so from now on. The model-dependent constants, s_ϕ and s_A can be easily estimated in the “central region” of the kink scalar profile [and were given after Eq. (28) for the “sine” superpotential, Eq. (14)]. In Fig. 5, we show the exact fermion zero-mode wavefunctions for several values of c to illustrate the situation in the benchmark scenarios defined in Subsection 2.3.3, with $k \gg m$. This allows us to characterize the physics of localization in close analogy to the standard treatment of bulk fermions in the Randall-Sundrum scenario. But note that, in general, Eq. (59) does not admit an exactly flat (“conformal”) zero-mode solution, since the y -dependence of the two terms in the exponent cannot cancel for all y ’s unless Eq. (60) holds.¹⁵ Also, the UV-localized wavefunctions have a Gaussian-like profile (see also [46, 47]), while the IR-localized wavefunctions have an exponential-like profile á la RS. Nevertheless, it is interesting that we end up dynamically in a limit where the RS intuition qualitatively holds. The approximate expression for the zero-mode profiles, Eq. (62), will be very useful in the following sections.

Going back to the heavy KK-mode fermion solutions, combining Eqs. (55) and (56) we obtain the decoupled system of second order differential equations:

$$f_L^{n''} - 2A' f_L^{n'} + \left[\frac{3}{4} A'^2 - \frac{1}{2} A'' - m_D A' + m'_D - m_D^2 + e^{2A} m_n^2 \right] f_L^n = 0 , \quad (63)$$

$$f_R^{n''} - 2A' f_R^{n'} + \left[\frac{3}{4} A'^2 - \frac{1}{2} A'' + m_D A' - m'_D - m_D^2 + e^{2A} m_n^2 \right] f_R^n = 0 . \quad (64)$$

In the absence of closed solutions for our chosen $A(y)$ and $m_D(y)$, one can find the spectrum (and wavefunctions) numerically by the “shooting method”.¹⁶ For instance, concentrating on f_L^n , one can integrate numerically Eq. (63) by starting at $y = -L$ with $f_L^n(-L) = 1$ and its derivative given by the first equation in (57). Varying $x_n = m_n/[k_{\text{eff}} e^{-A(L)}]$, one can

¹⁵This also shows that our background would break supersymmetry in a “hard way”, since the gaugino zero-mode profile, hence its couplings, cannot exactly match those of the gauge field.

¹⁶From a numerical perspective, it is easier to solve for $e^{-\frac{1}{2}A(y)} f_{L,R}^n$.

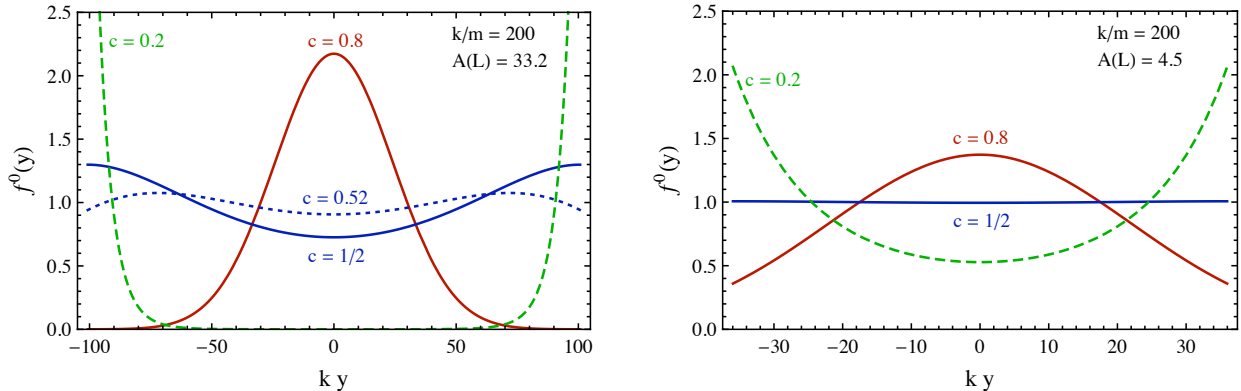


Figure 5: *Fermion zero-mode wavefunctions, Eq. (59), for the “strong warping” (left panel) and “small warping” (right panel) scenarios. The c -parameter is defined by Eq. (61). Note that the Randall-Sundrum intuition approximately applies, but there is no symmetry between UV and IR localized wavefunctions due to the approximately Gaussian warp factor. The dynamical UV brane is at $y = 0$, while $y = \pm L$ correspond to IR boundaries.*

find those values of x_n for which $f_L^{n'}(0) = 0$. These correspond to the even mode solutions. Similarly, the values of x_n that make $f_L^n(0) = 0$ determine the odd mode solutions. In practice, it is easier to find the even LH spectrum by solving Eq. (64) for f_R^n and requiring $f_R^n(0) = 0$, which by the first order Eq. (55) implies $f_L^{n'}(0) = 0$. This only misses the LH zero-mode solution, that we know explicitly from Eq. (59). We show in Fig. 6 the result of the above procedure for the “strong warping” benchmark scenario defined in Subsection 2.3.3, taking $c = 1/2$, so that the fermion zero mode is (approximately) flat. We use the exact profiles for $A(y)$ and $\phi(y)$ to generate the figure. However, to the extent that Eqs. (27) and (28) hold, this example corresponds to the “conformal” case, and the solutions for the x_n approximately coincide with those of (unbroken) gauge fields.¹⁷ Indeed, one can check that the gauge spectrum coincides with the one shown in the figure at the percent level. We note from the figure the high degree of degeneracy between the even and odd KK modes. This is due to the fact that the KK-mode wavefunctions are highly peaked near the IR boundaries, hence small changes in x_n allows one to change from $f_L^{n'}(0) = 0$ to $f_L^n(0) = 0$, turning an even mode into an odd mode (the same effect discussed for the radion/odd-scalar in Section 3). The degree of degeneracy increases as $A(L)$ increases.

As discussed above, there is always an even zero-mode. In addition, in certain regions of parameter space, there are light vector-like odd-modes that can be treated analytically, as we discuss in the next subsection.

4.2 Light Vector-like Odd Modes

For concreteness, in the following we concentrate on the case of a left-handed zero mode, i.e. we impose the boundary conditions of Eq. (57) [our results for the light mass and its

¹⁷Assuming vanishing brane-localized kinetic terms [48].

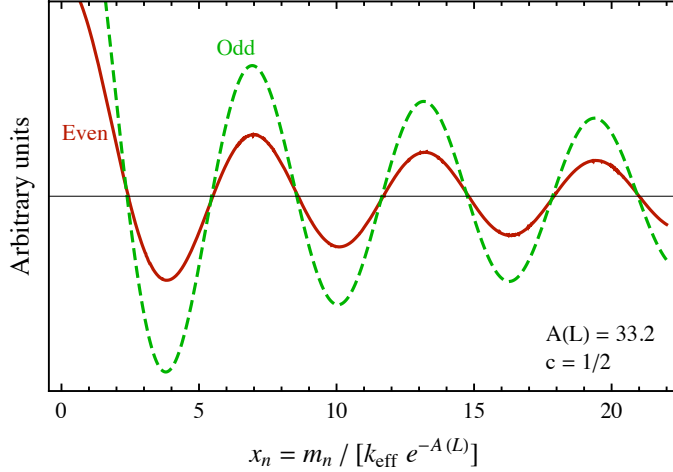


Figure 6: We plot $f_R(0)$ (solid, red curve) and $f_L(0)$ (dashed, green curve) as a function of $x_n = m_n/[k_{\text{eff}} e^{-A(L)}]$, for the boundary conditions of Eq. (57) [which select a LH zero-mode]. The zeros of $f_R(0)$ (which imply zeros of $f_L^1(0)$) correspond to the even mode LH solutions, while those of $f_L(0)$ correspond to the odd mode LH solutions. We choose $c = 1/2$ [approximately flat fermion zero-mode in the linear regime of Eqs. (27) and (28)], so that the roots also approximately correspond to those of gauge fields (see text). In this example, the roots are at $x_n^{\text{even}} \approx \{0, 2.43, 5.51, 8.60, 11.70, 14.80, \dots\}$ and $x_n^{\text{odd}} \approx \{2.38, 5.46, 8.55, 11.65, 14.75, \dots\}$. Notice the near degeneracy between the even and odd spectra.

wavefunction also hold when the zero-mode is right-handed, by a simple exchange of the labels $L \leftrightarrow R$]. In the case that the zero-mode fermion is exponentially localized near the IR boundaries, we expect to find an ultralight odd-fermion solution (for the same reasons as for the radion case discussed above). To find this small mass we write the wavefunction for the LH chirality of this odd-fermion (the first KK-mode), on the interval $[0, L]$, as $f_L^1(y) = f_L^0(y) + \epsilon(y)$, where f_L^0 is the (even) zero-mode profile given in Eq. (59) [$f_L^1(y)$ is completely fixed on the interval $[-L, 0]$ from the fact that it is odd about $y = 0$]. One then finds that Eq. (63) becomes

$$\epsilon'' - 2A'\epsilon' + \left[\frac{3}{4}A'^2 - \frac{1}{2}A'' - m_D A' + m_D' - m_D^2 + e^{2A} m_1^2 \right] \epsilon + e^{2A} m_1^2 f_L^0 = 0, \quad (65)$$

and requiring that the zero mode and the first excited mode have the same value at L we have the boundary conditions $\epsilon(L) = \epsilon'(L) = 0$.

We give an approximate solution for $\epsilon(y)$ in the limit that $\phi(y)$ and $A(y)$ are approximately given by Eqs. (27) and (28), respectively, and therefore Eq. (60) approximately holds (with the upper sign). Neglecting the $e^{2A} m_1^2 \epsilon$ term (which is smaller than the other terms proportional to ϵ provided $m_1 \ll k e^{-A(L)}$), Eq. (65) can be written as

$$e^{(c-\frac{1}{2})A} \partial_y \left\{ \partial_y \left[e^{(c-\frac{1}{2})A} \epsilon \right] e^{-(2c+1)A} \right\} = -m_1^2 f_L^0. \quad (66)$$

This can be integrated immediately to give

$$\epsilon(y) = -m_1^2 e^{-(c-\frac{1}{2})A(y)} \int_y^L dz_2 e^{(2c+1)A(z_2)} \int_{z_2}^L dz_1 e^{-(c-\frac{1}{2})A(z_1)} f_L^0(z_1), \quad (67)$$

where we imposed the boundary conditions given after Eq. (65). Requiring that $f_L^1(0) = f_L^0(0) + \epsilon(0) = 0$ determines the lightest odd-fermion mass as

$$m_1^2 \approx \left\{ \int_0^L dz_2 k_{\text{eff}} e^{(2c+1)A(z_2)-A(L)} \int_{z_2}^L dz_1 k_{\text{eff}} e^{-(c-\frac{1}{2})A(z_1)-A(L)} \frac{f_L^0(z_1)}{f_L^0(0)} \right\}^{-1} k_{\text{eff}}^2 e^{-2A(L)}, \quad (68)$$

where we used $A(0) = 0$. This form shows that the lightness of this odd mode is associated with $f_L^0(0)/f_L^0(L) \ll 1$. Indeed, since in the present limit the zero-mode profile is well approximated by Eq. (62), we can write

$$m_1^2 \approx \left\{ \int_0^L dz_2 k_{\text{eff}} e^{(2c+1)A(z_2)-A(L)} \int_{z_2}^L dz_1 k_{\text{eff}} e^{-(2c-1)A(z_1)-A(L)} \right\}^{-1} k_{\text{eff}}^2 e^{-2A(L)}. \quad (69)$$

This expression allows us to understand the suppression in m_1 compared to the natural KK scale $k_{\text{eff}} e^{-A(L)}$ when $c < 1/2$, i.e. when the zero-mode is IR localized and we expect a light odd-fermion mode [thus validating the approximation made above of neglecting the $e^{2A} m_1^2 \epsilon$ term in Eq. (66)]. In such a case, and using the approximation (28) for $A(y)$, the factor $e^{-(2c-1)A(z_1)}$ is localized near the IR boundary over a distance of order $[(1-2c)k_{\text{eff}}]^{-1}$, and therefore the z_1 integration can be restricted to the region $[L - \{(1-2c)k_{\text{eff}}\}^{-1}, L]$. To proceed further, it is useful to distinguish two cases:

- $-1/2 < c < 1/2$: the factor $e^{(2c+1)A(z_2)}$ is also localized towards the IR boundary, over a distance of order $[(2c+1)k_{\text{eff}}]^{-1}$. We can therefore restrict the integral over z_2 to the region $[L - \{(1+2c)k_{\text{eff}}\}^{-1}, L]$. With this restriction over z_2 we find that the effective support of the z_1 integration is of order $(2k_{\text{eff}})^{-1}$, in the vicinity of $z_1 = L$. Evaluating all the exponentials at L , we then get

$$m_1 \approx \sqrt{2(1+2c)} k_{\text{eff}} e^{-A(L)}, \quad (70)$$

where we recall that $k_{\text{eff}} = A'(L) = s_A k$.

- $c < -1/2$: the factor $e^{(2c+1)A(z_2)}$ is now localized near $y = 0$. The integral over z_1 can then be evaluated from 0 to L for all z_2 , giving a factor $[(1-2c)k_{\text{eff}}]^{-1} e^{-2cA(L)}$. For $|c| \sim \mathcal{O}(1)$, the integral over z_2 can then be estimated as an average and gives $L e^{-A(L)} (1/2) [e^{(2c+1)A(L)} + e^{(2c+1)A(0)}]$. Putting these together, we have

$$m_1 \approx \sqrt{\frac{2(1-2c)}{k_{\text{eff}} L} \frac{1}{1 + e^{-(2c+1)A(L)}}} k_{\text{eff}} e^{-A(L)}, \quad (71)$$

where we used $A(0) = 0$. This shows that for extreme localization of the zero-mode solution, i.e. for $2c+1$ very negative, the lightest odd-fermion mode has an exponentially small mass, where $m_1/(k_{\text{eff}} e^{-A(L)}) \sim e^{(c+\frac{1}{2})A(L)}$.

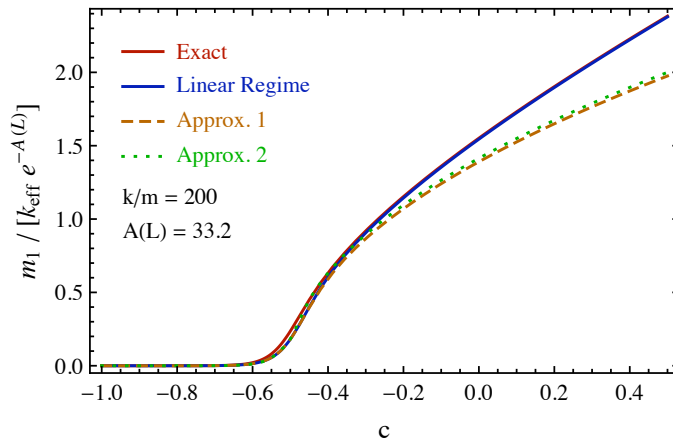


Figure 7: *Lightest odd-fermion mass (in units of $k_{\text{eff}} e^{-A(L)}$) as a function of c . The solid (red) line corresponds to the numerical result with the exact scalar and warp factor profiles of Eqs. (15) and (16). The solid (blue) line corresponds to the numerical solution but with $\phi(y)$ and $A(y)$ given by Eqs. (27) and (28) (the “linear regime”). The dashed (brown) line corresponds to the approximation of Eq. (69) (“Approx. 1”). The dotted (green) line corresponds to Eqs. (70) and (71) (“Approx. 2”).*

In Fig. 7, we show the lightest odd-fermion mass (in units of $k_{\text{eff}} e^{-A(L)}$) as a function of c for the approximation given in Eq. (69) with $A(y) = k_{\text{eff}} y^2 / (2L)$ [dashed, brown line], and for Eqs. (70) and (71) in the regions $-1/2 < c < 1/2$ and $c < -1/2$, respectively [dotted, green line].¹⁸ We also show the exact result (with the exact warp factor and scalar profile) obtained by numerical integration (solid, red line), as well as the exact numerical solution but assuming that $\phi(y)$ and $A(y)$ are precisely given by Eqs. (27) and (28) (solid, blue line). We restrict to the “strong warping” scenario, with $k/m = 200$ (see Subsection 2.3.3). We see that the simple expressions derived above are fairly reasonable whenever $m_1 / (k_{\text{eff}} e^{-A(L)}) \lesssim 1$.

For later use, we also give here the wavefunctions for the two chiralities of the first (KK-parity odd) fermion KK mode. The left-handed chirality (or more generally, the chirality that coincides with that of the zero-mode fermion in the tower) was found before in terms of $\epsilon(y)$ of Eq. (67) on the interval $[0, L]$. Allowing for a normalization factor N_1 , to be determined from Eq. (54), we have for $y > 0$:

$$f_L^1(y) \approx N_1 e^{(\frac{1}{2}-c)A(y)} \left[1 - m_1^2 \int_y^L dz_2 e^{2A(z_2)} \left(\frac{f^0(z_2)}{f^0(0)} \right)^{-2} \int_{z_2}^L dz_1 \left(\frac{f^0(z_1)}{f^0(0)} \right)^2 \right], \quad (72)$$

where f^0 is the zero-mode wavefunction as given in Eq. (62). For $y < 0$ one uses $f_L^1(-y) = -f_L^1(y)$. The wavefunction for the right-handed chirality (more generally, the chirality opposite to that of the zero-mode in the tower) is obtained from Eq. (55). Using that $e^{(\frac{1}{2}-c)A(y)}$

¹⁸The approximation of Eq. (70) fails at $c = -1/2$, since the factor $e^{(2c+1)A(z_2)}$ becomes constant. However, numerically the approximation works rather well down to $c \simeq -0.48$. For the dotted green line in Fig. 7 we interpolated linearly between Eq. (70) at $c = -0.48$ and Eq. (71) at $c = -0.5$.

is the massless solution of Eq. (55) [in the linear limit], f_R^1 is given on the interval $[0, L]$ by

$$f_R^1(y) \approx -N_1 m_1 e^{(\frac{1}{2}+c)A(y)} \int_y^L dz \left(\frac{f^0(z)}{f^0(0)} \right)^2, \quad (73)$$

which explicitly satisfies $f_R^1(L) = 0$. For $y < 0$ one uses $f_R^1(-y) = +f_R^1(y)$, i.e. that this wavefunction is even under $y \rightarrow -y$.¹⁹ To the extent that $m_1 \ll k_{\text{eff}} e^{-A(L)}$, we have that $\epsilon(y)$ is a small effect and therefore the normalization constant N_1 coincides approximately with the normalization of the zero mode:

$$N_1 \approx N_0 \approx \sqrt{\frac{2(1-2c)A(L)}{e^{(1-2c)A(L)} - 1}}, \quad (74)$$

where we used the approximate expression for the warp factor, Eq. (28) [see Eq. (86) below for more details of the evaluation of N_0].

5 The Higgs Field and EWSB

The action for a (for simplicity, real) bulk scalar H takes the form:

$$S_{\text{scalar}} = \int d^5x \sqrt{g} \left\{ \frac{1}{2} g^{MN} \partial_M H \partial_N H - V(H) + \delta(y+L) \mathcal{L}_{-L} + \delta(y-L) \mathcal{L}_{+L} \right\}, \quad (75)$$

where we allow for IR brane localized terms $\mathcal{L}_{\pm L}$ (these δ -terms should be written with the induced metric, but since in our background we have $\sqrt{g} = \sqrt{g_{\text{ind}}}$, we have omitted this distinction for notational simplicity). Focusing on the quadratic terms, $V(H) = \frac{1}{2} M^2 H^2 + \dots$, the KK decomposition is written as

$$H(x^\mu, y) = \frac{e^{A(y)}}{\sqrt{2L}} \sum_{n=0}^{\infty} H_n(x^\mu) f_n(y), \quad (76)$$

where the KK wavefunctions obey

$$f_n'' - 2A' f_n' + [A'' - 3A'^2 - M^2 + e^{2A} m_n^2] f_n = 0, \quad (77)$$

and are normalized according to

$$\frac{1}{2L} \int_{-L}^L dy f_n(y) f_m(y) = \delta_{nm}. \quad (78)$$

The boundary conditions associated with localized mass terms $\mathcal{L}_{\pm L} = -\frac{1}{2} M_{\pm L} H^2$, where KK-parity imposes $M_{-L} = M_{+L}$, read

$$f_n' + (A' \pm M_{\pm L}) f_n \Big|_{\pm L} = 0. \quad (79)$$

¹⁹Since at $y = 0$ we have $m_D = 0$ and $A' = 0$, the fermion equations of motion (55) and (56) imply that if one of the two chiralities has vanishing first derivative at $y = 0$ (an even mode) then the opposite chirality vanishes at $y = 0$ (an odd mode), and viceversa.

It is convenient to parameterize the bulk and brane masses by

$$M^2 = (\alpha^2 - 4) k_{\text{eff}}^2, \quad M_{\pm L} = (\alpha - 2) k_{\text{eff}} + m_{\pm L}. \quad (80)$$

where $k_{\text{eff}} \equiv A'(L)$, $\alpha \equiv c + 1/2$, and $c = m_D(L)/A'(L)$ as defined in Eq. (61) [see also Eqs. (27) and (28)]. In the AdS₅ limit, where $A(y) = ky$, these equations admit a zero-mode solution when $m_{\pm L} = 0$. This follows by comparison with the KK fermion Eq. (63), and the boundary condition (57). The zero-mode localization is controlled by the same c -parameter that characterizes the fermion case.

We point out that for modes that are highly localized near the IR boundaries, so that in the region $y > 0$ we can replace $A'(y) \approx A'(L) = k_{\text{eff}}$ and $A''(y)/k_{\text{eff}}^2 \approx 1/(k_{\text{eff}}L) \approx 1/[2A(L)] \ll 1$, Eq. (77) reduces to the fermion Eq. (63) with $m_D(y) \approx m_D(L) = cA'(L)$. The scalar and fermion boundary conditions also coincide in this case, up to the terms $m_{\pm L}$. Thus, when $c \ll 1/2$ (strong fermion zero-mode localization in the IR), the scalar EOM also has a light mode, whose mass is controlled by $m_{\pm L}$. To the extent that $m_{\pm L}$ is small, the scalar and fermion spectra almost coincide in this extreme IR localized limit. In particular, from the same considerations discussed in the radion and fermion cases of the previous sections, there is a KK-parity odd mode that is exponentially degenerate with the lightest scalar (KK-parity even) mode.

5.1 Electroweak Symmetry Breaking

A natural solution to the hierarchy problem suggests that the Higgs field is localized near the IR boundaries. In this case, the Higgs KK modes become heavy and decouple, except for the lightest KK-parity even and odd modes. If the Higgs had a vanishing VEV, the discussion of the previous section would imply that these two light states are nearly degenerate, with their masses controlled by the boundary mass terms $m_{\pm L}$ introduced above. However, we need to introduce a potential that leads to EWSB. It must also not break KK-parity, which implies that only the KK-parity even Higgs mode can acquire a non-zero VEV. The potential can arise from bulk or from IR localized terms, but we may simply analyze the physics of EWSB in the low-energy 4D effective theory. The relevant 4D degrees of freedom are KK-parity even and odd $SU(2)$ doublets with hypercharge +1, that can be parameterized, respectively, as

$$H_+ = \begin{pmatrix} G^+ \\ \tilde{v} + \frac{1}{\sqrt{2}}h_+ + \frac{i}{\sqrt{2}}G^0 \end{pmatrix}, \quad H_- = \begin{pmatrix} H^+ \\ \frac{1}{\sqrt{2}}h_- + \frac{i}{\sqrt{2}}a \end{pmatrix}, \quad (81)$$

where \tilde{v} denotes the warped-down VEV. Besides the kinetic terms, $D_\mu H_+^\dagger D^\mu H_+ + D_\mu H_-^\dagger D^\mu H_-$, we can get potential terms of the form

$$\begin{aligned} V = & m_{\text{odd}}^2 H_-^\dagger H_- + \frac{1}{2} \lambda_1 (H_-^\dagger H_-)^2 + \frac{1}{2} \lambda_2 (H_+^\dagger H_+ - \tilde{v}^2)^2 + \lambda_3 (H_-^\dagger H_-) (H_+^\dagger H_+ - \tilde{v}^2) \\ & + \lambda_4 (H_+^\dagger H_-) (H_-^\dagger H_+) + \frac{1}{2} \lambda_5 \left[(H_+^\dagger H_-)^2 + (H_-^\dagger H_+)^2 \right], \end{aligned} \quad (82)$$

where m_{odd}^2 is the light KK mass discussed in the previous subsection. The above potential terms lead to masses $m_{h_+}^2 = 2\lambda_2\tilde{v}^2$, $m_{h_-}^2 = m_{\text{odd}}^2 + (\lambda_4 + \lambda_5)\tilde{v}^2$, $m_a^2 = m_{\text{odd}}^2 + (\lambda_4 - \lambda_5)\tilde{v}^2$, and $m_{H^\pm}^2 = m_{\text{odd}}^2$ (G^0 and G^\pm are the eaten would-be Goldstone bosons).

We note here, for later reference, that the KK-parity odd “kinetic terms”, $D_\mu H_+^\dagger D^\mu H_- + D_\mu H_-^\dagger D^\mu H_+$, as well as the KK-parity odd potential terms, $\lambda_6(H_+^\dagger H_- + H_-^\dagger H_+)(H_+^\dagger H_+ + \zeta H_-^\dagger H_- - \tilde{v}^2)$ can also appear, for instance when coupled to a KK-parity odd radion excitation, r'/Λ_r . For strongly IR localized Higgs fields we expect $\lambda_1 \approx \dots \approx \lambda_6$ and $\zeta \approx 1$.

5.2 Yukawa Couplings to the Higgs and SM Fermion Masses

We consider next the fermion Higgs interactions. Consider the top Yukawa interaction

$$\delta S = - \int d^5x \sqrt{g} \left[\tilde{Y}_{5D} H \bar{Q} t + h.c. \right], \quad (83)$$

where \tilde{Y}_{5D} is the 5D Yukawa coupling (with mass dimension $-1/2$), H is the bulk Higgs doublet, Q is the third generation quark $SU(2)$ doublet, and t is the top $SU(2)$ singlet [Q satisfies the b.c.’s given in Eq. (57) and t those given in Eq. (58)].

Focusing on the zero-mode fermions, as defined by Eq. (53), the effective 4D Yukawa coupling reads

$$Y_{4D} = \frac{\tilde{Y}_{5D}}{(2L)^{3/2}} \int_{-L}^L dy f_{h_+}(y) f_L^0(y) f_R^0(y) \approx \frac{Y_{5D}}{L} f_L^0(L) f_R^0(L), \quad (84)$$

where we took into account that the fermion zero-modes, as well as f_{h_+} , are even about $y = 0$, and the second equality holds in the limit where the lightest Higgs state is strongly IR localized over a distance of order k_{eff} , so that $f_{h_+}(L) \approx \sqrt{k_{\text{eff}}L}$. We also defined a 5D Yukawa coupling $Y_{5D} = \tilde{Y}_{5D}/\sqrt{2k_{\text{eff}}}$, as would be appropriate for a localized Higgs field. The general fermion zero-mode profiles are given in Eq. (59), but here we use the approximations given in Eq. (62) with the warp factor given in Eq. (28). Recall that we use conventions such that for $c > 1/2$ ($c < 1/2$) the zero-mode fermion is UV (IR) localized, independently of chirality. In addition, it is useful to write simple analytical expressions for the properly normalized wavefunctions that hold in the limit that $A(L) \gg 1$. For $c > 1/2$ we use the fact that for $z \gg 1$ one has $\int_0^z dp e^{-p^2} \approx \sqrt{\pi}/2$, so that Eq. (62) reads

$$f^0(y) \approx \left[\frac{8(c - \frac{1}{2})A(L)}{\pi} \right]^{1/4} e^{-(c - \frac{1}{2})A(y)}, \quad \text{for } c > 1/2. \quad (85)$$

For $c < 1/2$ one has instead $\int_0^z dp e^{p^2} \approx \frac{1}{2z} e^{z^2}$ whenever $z \gg 1$, and therefore

$$f^0(y) \approx \sqrt{\frac{4(\frac{1}{2} - c)A(L)}{e^{(1-2c)A(L)}}} e^{(\frac{1}{2} - c)A(y)}, \quad \text{for } c < 1/2. \quad (86)$$

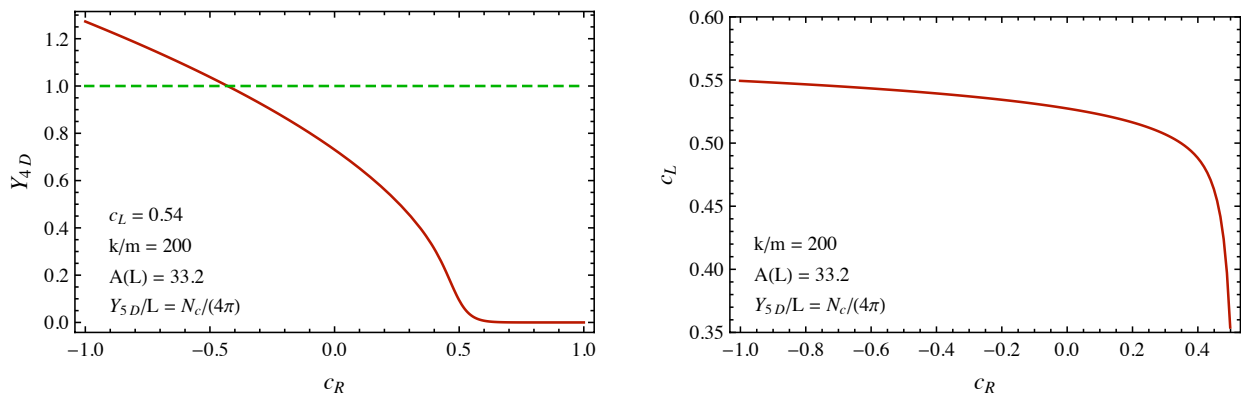


Figure 8: *Left panel:* Four-dimensional Yukawa coupling as a function of c_R , for fixed $c_L = 0.54$, $k/m = 200$ and $A(L) = 33.2$. The dashed (green) line shows the approximate value of the top Yukawa coupling which occurs for $c_R \sim -0.45$. *Right panel:* c_L as a function of c_R for the observed top mass ($Y_{4D} \approx 1$), assuming $Y_{5D} = N_c/(4\pi)$, with $N_c = 3$.

These approximations work extremely well except very close to $c = 1/2$, where the wavefunction is (approximately) flat: $f^0(y) \approx 1$. Then, for instance, if the LH top has a flat profile ($c_L = 1/2$), while the RH top is localized near the IR boundaries ($c_R < 1/2$) the 4D top Yukawa coupling reads

$$Y_{4D} \approx \sqrt{(1 - 2c_R) k_{\text{eff}} L} \times \frac{Y_{5D}}{L}, \quad (87)$$

where we used Eq. (28) for $A(L)$.

We estimate the maximum value of Y_{5D} from Naive Dimensional Analysis (NDA) in extra dimensions with singularities [45]. Writing the 5D Yukawa coupling as $Y_{5D} = w/\Lambda_5$, where Λ_5 is the cutoff scale of the 5D theory, NDA gives $w_{\text{NDA}} \sim l_5/\sqrt{l_4}$, where $l_5 = 24\pi^3$ and $l_4 = 16\pi^2$ are the 5D and 4D loop factors, respectively. Also, taking Λ_5 as the scale where 5D QCD gets strong gives

$$\Lambda_5 L \sim l_5/N_c, \quad (88)$$

where $N_c = 3$ is the number of colors. Therefore, we estimate

$$\frac{Y_{5D}^{\text{NDA}}}{L} \sim \frac{N_c}{\sqrt{l_4}} = \frac{3}{4\pi}. \quad (89)$$

In the left panel of Fig. 8 we show the top Yukawa coupling as a function of c_R for $c_L = 0.54$, taking Y_{5D} as given in Eq. (89) [and in the “strong warping” benchmark scenario of Subsection 2.3.3]. We use the exactly normalized zero-mode fermion profiles, although the approximate formulas given above lead to very accurate results except in the close vicinity of $c = 1/2$. Notice that we can generate a 4D Yukawa coupling of order one with a flat –or even slightly localized on the UV brane ($c_L \sim 0.54$)– left-handed zero mode, and a right-handed zero mode near the IR brane ($c_R \sim -0.45$). For these values, Fig. 7 shows that there is a KK-parity odd resonance of the $SU(2)$ singlet top with a mass $m_1 \sim 0.44 \tilde{k}_{\text{eff}}$.

In the right panel of Fig. 8, we show the required c_L as a function of c_R , that reproduces the observed 4D top Yukawa coupling, again assuming that the 5D Yukawa coupling takes the NDA value of Eq. (89). We see that the $SU(2)$ top doublet has $c_L \sim 0.5$, except when c_R approaches $1/2$.

6 Gauge Fields

For completeness, we summarize here the KK decomposition for gauge fields (in the absence of brane kinetic terms). The results apply for general diagonal metrics of the form (2). The gauge action reads

$$S = \int d^5x \sqrt{g} \left\{ -\frac{1}{4} g^{MK} g^{NL} F_{MN} F_{KL} \right\} + S_{\text{g.f.}} . \quad (90)$$

The gauge fixing term in the background of Eq. (2) is chosen as [49]

$$S_{\text{g.f.}} = -\frac{1}{2\xi} \int d^5x \left\{ \partial_\mu V^\mu - \xi \partial_y [e^{-2A} V_5] \right\}^2 , \quad (91)$$

where ξ is the gauge fixing parameter, and the 4D indices are contracted with $\eta_{\mu\nu}$. The KK mode expansions then read

$$V_{\mu,5}(x, y) = \frac{1}{\sqrt{2L}} \sum_{n=0}^{\infty} V_{\mu,5}^n(x) f_{V,5}^n(y) , \quad (92)$$

where

$$\partial_y [e^{-2A} \partial_y f_V^n] + m_n^2 f_V^n = 0 , \quad (93)$$

and $f_5^n = \partial_y f_V^n / m_n$. For SM gauge fields, the boundary conditions are taken as $\partial_y f_V^n|_{0,L} = f_5^n|_{0,L} = 0$, so that there is no zero-mode for V_5 . In the above R_ξ -type of gauge, V_5^n has mass ξm_n^2 . The KK wavefunctions obey the orthonormality relation

$$\frac{1}{2L} \int_{-L}^L dy f_V^n f_V^m = \delta_{nm} . \quad (94)$$

The gauge eigenvalues in the “strong warping” benchmark scenario defined in Subsection 2.3.3 are approximately given in Fig. 6. The gauge zero-mode wavefunction, however, is always exactly flat ($f_V^0 = 1$), unlike the zero-mode wavefunction for a fermion with $c = 1/2$.

7 Radion and KK-Radion Couplings at Linear Order

In previous sections we saw that, apart from the “zero-mode” sector (that includes the SM fields plus the radion), some first-level KK states can be relatively light compared to the KK

scale. These light states are KK-parity odd. In particular, in the present scenario the lightest KK-parity odd particle (the LKP) is the first level KK-radion while the second lightest KK state (the NLKP) corresponds to either the first KK-parity odd mode of the IR localized top $SU(2)$ singlet, or the first KK-parity odd excitation of the Higgs doublet. In this section, we work out the Feynman rules for the interactions involving a radion/KK-radion with the top KK tower, and give some numerical examples. We also give the radion/KK-radion couplings to the gauge KK towers, and also to the two Higgs doublets.

7.1 KK-Radion Couplings to Fermions

The couplings of the radion KK tower to the KK fermions are obtained by replacing into the action the KK decompositions for the metric and bulk scalar, as given in Eqs. (29)-(32), together with the fermion KK decomposition given in Eq. (53). We are interested in the terms linear in the radion or its first KK-parity odd excitation.²⁰ There are two types of contributions. First, those arising from the bulk fermion action, Eq. (52), which involve KK fermions belonging to the same 5D fermion field. Second, those arising from the localized Yukawa interactions, as in Eq. (83), which involve KK fermions belonging to different 5D fermion fields.

The Yukawa interactions lead to mass mixing (after EWSB) between different fermion KK towers, most importantly for the top tower. Although these effects can be taken into account perturbatively, it is safer to perform a KK decomposition that already incorporates EWSB effects (for an IR-localized Higgs field, the bulk solutions worked out before do not change, but the boundary conditions are deformed by EWSB). In this way, the effects of EWSB appear directly in the vertices and spectrum, and one does not have to worry about mixing in external legs of physical processes. A second possibility is to diagonalize the fermion mass matrix including a sufficiently large number of KK modes. Here, for simplicity, we will derive the Feynman rules for the vertices *ignoring* EWSB. This should contain the essential physics for most applications (but see Ref. [29] for a discussion of EWSB effects). However, note that the localized Yukawa terms also lead to quartic interactions involving the physical Higgs, h , of the form $h-r_i-t^j-t^k$ that are proportional to the EWSB zero-mode fermion mass, m_t .

As just stated, we proceed now by setting EWSB to zero. In terms of the canonically normalized radion KK modes, $r_n(x) \equiv \Lambda_r \tilde{r}_n(x)$, where Λ_r is the radion decay constant defined in Eq. (38), the interactions induced by the bulk action take the form

$$\mathcal{L}_{r\psi\psi}^{\text{bulk}} = - \sum_{ijk=0}^{\infty} \frac{r_i}{\Lambda_r} \left[g_{ijk}^{LL} \bar{\psi}_L^j i \overleftrightarrow{\not{\partial}} \psi_L^k + g_{ijk}^{RR} \bar{\psi}_R^j i \overleftrightarrow{\not{\partial}} \psi_R^k \right] + \sum_{ijk=0}^{\infty} \frac{r_i}{\Lambda_r} [m_{ijk}^{RL} \bar{\psi}_R^j \psi_L^k + \text{h.c.}] , \quad (95)$$

²⁰Note that the couplings involving heavier radion KK states receive a further suppression from the $1/m_n^2$ in the radion normalization, Eq. (36) [in other words, heavier radion modes have an effectively larger decay constant, $\Lambda_r^n \sim x_n \Lambda_r$, where $m_n = x_n k_{\text{eff}} e^{-A(L)}$ is the n -th KK radion mass].

where $\bar{\psi} \overleftrightarrow{\partial} \chi \equiv \frac{1}{2} [\bar{\psi} \gamma^\mu \partial_\mu \chi - (\partial_\mu \bar{\psi}) \gamma^\mu \chi]$,

$$g_{ijk}^{LL} = \frac{1}{2L} \int_{-L}^L dy F_i f_L^j f_L^k, \quad g_{ijk}^{RR} = \frac{1}{2L} \int_{-L}^L dy F_i f_R^j f_R^k, \quad (96)$$

$$m_{ijk}^{RL} = 2g_{ijk}^{LL} m_j + 2g_{ijk}^{RR} m_k - \frac{1}{2L} \int_{-L}^L dy e^{-A} \left[2m_D F_i + \frac{m'_D}{A''} e^{2A} (e^{-2A} F_i)' \right] f_R^j f_L^k, \quad (97)$$

and $m_{ijk}^{LR} = m_{ikj}^{RL}$. Here we have used the fact that the fünfbein is diagonal with $e_\nu^\mu \approx e^A (1 + F) \delta_\nu^\mu$ and $e_5^5 \approx (1 - 2F)$. To arrive at Eq. (97) we used the fermion equations of motion, Eq. (55) and (56). The second term in the integral in Eq. (97) arises from the scalar fluctuations given in Eq. (31), where we used the background relation $\phi'^2 = 3M_5^3 A''$ to eliminate M_5 . Note also that the integrands in Eq. (96) and Eq. (97) are odd when $(i + j + k) \neq 0 \pmod{2}$, which implies $g_{ijk}^{LL} = g_{ijk}^{RR} = m_{ijk}^{RL} = 0$ in such cases, so that KK-parity is not violated.

It is of some interest to consider the interactions involving n radion modes and a fermion pair. The $r_{i_1} \cdots r_{i_n} \bar{\psi}^j \psi^k$ interactions take a similar form to Eq. (95) with $\Lambda_r \rightarrow \Lambda_r^n$, $g_{ijk}^{LL} \rightarrow c_n g_{i_1 \dots i_n jk}^{LL}$, $g_{ijk}^{RR} \rightarrow c_n g_{i_1 \dots i_n jk}^{RR}$ and $m_{ijk}^{RL} \rightarrow d_n m_{i_1 \dots i_n jk}^{RL}$, where $c_n = (-3)^n (2n/3 - 1)/n!$ and $d_n = (-4)^{n-1}/n!$ are combinatorial factors, and

$$\begin{aligned} g_{i_1 \dots i_n jk}^{LL} &= \frac{1}{2L} \int_{-L}^L dy F_{i_1} \cdots F_{i_n} f_L^j f_L^k, & g_{i_1 \dots i_n jk}^{RR} &= \frac{1}{2L} \int_{-L}^L dy F_{i_1} \cdots F_{i_n} f_R^j f_R^k, \quad (98) \\ m_{i_1 \dots i_n jk}^{RL} &= 2g_{i_1 \dots i_n jk}^{LL} m_j + 2g_{i_1 \dots i_n jk}^{RR} m_k - \frac{1}{L} (2 - n) \int_{-L}^L dy e^{-A} m_D F_{i_1} \cdots F_{i_n} f_R^j f_L^k \\ &\quad - \frac{1}{2L} \frac{n}{2} (3 - n) \int_{-L}^L dy \frac{m'_D}{A''} e^A F_{i_1} \cdots F_{i_{n-1}} (e^{-2A} F_{i_n})' f_R^j f_L^k. \end{aligned} \quad (99)$$

It is understood that in the Lagrangian we write separate terms for each (i_1, \dots, i_n) ordered n -tuple. For instance, in the case $n = 2$, if $i_1 \neq i_2$ we have two terms corresponding to $r_{i_1} r_{i_2} \bar{\psi}^j \psi^k$ and $r_{i_2} r_{i_1} \bar{\psi}^j \psi^k$, with the coefficients given above. If $i_1 = i_2$ then there is a single term. This case plays a role in the annihilation processes $r_i r_i \rightarrow \bar{\psi} \psi$.

The bulk action also leads to interactions involving the radion, fermion pairs and gauge bosons V_μ of the form

$$\mathcal{L}_{r\psi\psi V} = - \sum_{ijkl} \frac{r_i}{\Lambda_r} (g_{ijkl}^{LL} \bar{\psi}_L^j \mathcal{V}^l \psi_L^k + g_{ijkl}^{RR} \bar{\psi}_R^j \mathcal{V}^l \psi_R^k), \quad (100)$$

where we used the KK expansion for the gauge fields, Eq. (92), and defined

$$g_{ijkl}^{LL} = \frac{g_V}{2L} \int_{-L}^L dy F_i f_L^j f_V^l f_L^k, \quad (101)$$

$$g_{ijkl}^{RR} = \frac{g_V}{2L} \int_{-L}^L dy F_i f_R^j f_V^l f_R^k, \quad (102)$$

with $g_V = g_{5V}/\sqrt{2L}$ the 4D gauge coupling. We work in unitary gauge so that there is no $\bar{\psi}_L^j V_5 \psi_R^k$ interaction (the V_5 components of the gauge field are eaten by the higher KK modes, and the zero-mode of V_5 is projected out by the boundary conditions). Note that when we consider the interactions involving a zero-mode gauge boson, with $f_V^0(y) = 1$ up to EWSB effects, we have $g_{ijkl}^{LL} = g_V g_{ijkl}^{LL}$ and $g_{ijkl}^{RR} = g_V g_{ijkl}^{RR}$, where g_{ijkl}^{LL} and g_{ijkl}^{RR} are defined in Eq. (96).

The Feynman rules for a single radion state, r_i , and two KK fermions or a pair of KK fermions and a (neutral) gauge boson are then

$$\begin{aligned}
 \begin{array}{c} \text{---} r_i \text{---} \\ \nearrow \text{---} \bar{t}^j \text{---} \\ \text{---} p_f \\ \searrow \text{---} t^k \text{---} \\ \text{---} p_i \end{array} &= -\frac{i}{\Lambda_r} \left\{ \frac{1}{2} (\not{p}_i + \not{p}_f) (g_{ijkl}^{LL} P_L + g_{ijkl}^{RR} P_R) - m_{ijk}^{RL} P_L - m_{ijk}^{LR} P_R \right\} , \\
 \begin{array}{c} \text{---} r_i \text{---} \\ \nearrow \text{---} \bar{t}_b^j \text{---} \\ \searrow \text{---} t_c^k \text{---} \\ \text{---} V_\mu^{l,a} \end{array} &= -\frac{i}{\Lambda_r} \gamma^\mu (T^a)_{bc} (g_{ijkl}^{LL} P_L + g_{ijkl}^{RR} P_R) ,
 \end{aligned}$$

which, as mentioned above, are non-vanishing only when $(i + j + k) = 0 \pmod{2}$, or $(i + j + k + l) = 0 \pmod{2}$. For the Feynman rule involving the gauge boson: in the case of the photon, $(T^a)_{bc} \rightarrow 1$ and $g_V = Q_t e$, with $Q_t = \frac{2}{3}$ the top quark electric charge; for the Z gauge boson, $(T^a)_{bc} \rightarrow 1$ and $g_V = \sqrt{g^2 + g'^2} (T_t^3 - Q_t s_W^2)$; for the gluons, $g_V = \sqrt{4\pi\alpha_s}$, with T^a the $SU(3)$ generators normalized according to $\text{Tr}(T^a T^b) = \frac{1}{2} \delta^{ab}$, and a, b, c are color indices.

The vertices involving the lightest states (the radion, the first KK radion, the RH top and its first KK excitation) are especially important, and their Feynman rules can be further simplified. We can also restrict to couplings involving the zero-mode gauge bosons. Since the radion, r [i.e. the lightest of the scalar fluctuations in the 5D metric/bulk scalar system, with a mass m_0 as given in Eqs. (43)-(45)], is KK-parity even, it can only couple to a pair of KK-parity even or a pair of KK-parity odd fermions. Similarly, the first radion excitation [which we call r' and is essentially degenerate with r (see Section 3)], is KK-parity odd and can couple to t and t' , where we denote by t' the first KK excitation of the $SU(2)$ singlet top. The couplings involving these light fields can be approximated based on the following observations:

1. The radion wavefunction is highly peaked near the IR boundaries over a distance of order $1/k_{\text{eff}}$, as given in Eq. (46). Also, as discussed in Section 4.2, r' has a wavefunction essentially identical to that of the radion: $F_1(y) \approx F_0(y)$.
2. For the RH top, $f_R^1(y) \approx f_R^0(y)$ on the interval $[0, L]$, and both the zero-mode and its first KK excitation, t' , are highly peaked near the IR boundaries. Recall that $f_R^0(y)$ was given in Eq. (86).

3. The wavefunction for the LH chirality of t' , $f_L^1(y)$ [given in Eq. (73), with the trivial change in label $R \rightarrow L$] is more spread-out over the full extent of the extra-dimension. To see this, note that the IR localization of $f_R^0(y)$ implies that the integral in Eq. (73) is almost y -independent, except very close to $y = L$, where it vanishes. Hence the main source of y -dependence arises from the $e^{(\frac{1}{2}+c_R)A(y)}$ factor. For $c_R \sim -1/2$ this factor is also nearly constant, so that the normalization implies that $f_L^1(y) \approx 1$.

It follows that for $c_R \sim -1/2$ the couplings involving $f_R^0(y)$ or $f_R^1(y)$ are larger than those involving $f_L^1(y)$ by a factor of order $f_R^0(L) \sim \sqrt{2(1-2c_R)A(L)} \sim \sqrt{k_{\text{eff}}L}$, for each occurrence of the RH versus LH wavefunction, so that for instance $g_{101}^{LL} \sim g_{101}^{RR}/(k_{\text{eff}}L)$ in Eq. (96). When c_R is not so close to $-1/2$ the suppression is less severe, but we still have $g_{101}^{LL} \ll g_{101}^{RR}$ provided $f_R^0(y)$ is IR localized. The integral in Eq. (97) is similarly suppressed. In fact, the second term inside the integral goes like $e^{-A}g'F_0f_R^0f_L^1$, where g' , as given in Eq. (42), gives an additional suppression that makes this contribution arising from the scalar fluctuations completely negligible. When focusing on the couplings to the lightest top KK state, we can therefore neglect all the contributions that depend on $f_L^1(y)$. For typical choices of parameters the errors thus induced are of order (10–20)%.

The upshot is that the bulk interactions between the radion/LKP, the NLKP (with both RH and LH chiralities) and the top quark, as well as those involving a SM gauge boson, are controlled by

$$g_{000}^{RR} \approx g_{011}^{RR} \approx g_{101}^{RR} = g_{110}^{RR} \approx \left(\frac{1-2c}{3-2c} \right) s_A^{1/2}. \quad (103)$$

For the radion couplings to a fermion pair, the explicit Feynman rules are:

$$\begin{array}{c} \text{---} r \text{---} \\ \diagup \quad \diagdown \\ p_f \quad \bar{t} \\ \diagdown \quad \diagup \\ p_i \quad t \end{array} \approx -i \frac{g_{000}^{RR}}{\Lambda_r} \frac{1}{2} (\not{p}_i + \not{p}_f), \quad (104)$$

$$\begin{array}{c} \text{---} r \text{---} \\ \diagup \quad \diagdown \\ p_f \quad \bar{t}' \\ \diagdown \quad \diagup \\ p_i \quad t' \end{array} \approx -i \frac{g_{011}^{RR}}{\Lambda_r} \left[\frac{1}{2} (\not{p}_i + \not{p}_f) P_R - 2m_{t'} \right]. \quad (105)$$

The mass of the first KK resonance, $m_{t'}$, is given in Eq. (70). Similarly, the couplings involving r' are:

$$\begin{array}{c} \text{---} r' \text{---} \\ \diagup \quad \diagdown \\ p_f \quad \bar{t}' \\ \diagdown \quad \diagup \\ p_i \quad t' \end{array} \approx -i \frac{g_{101}^{RR}}{\Lambda_r} \left[\frac{1}{2} (\not{p}_i + \not{p}_f) P_R - 2m_{t'} P_L \right], \quad (106)$$

$$\approx -i \frac{g_{101}^{RR}}{\Lambda_r} g_V \gamma^\mu (T^a)_{bc} P_R, \quad (107)$$

where V_μ stands for any of the neutral SM gauge bosons. We did not write explicitly the hermitian conjugate processes. The rules for the $V_\mu - r - t - \bar{t}$ and $V_\mu - r - t' - \bar{t}'$ vertices are analogous to Eq. (107), with $g_{101}^{RR} \rightarrow g_{000}^{RR}$ and $g_{101}^{RR} \rightarrow g_{011}^{RR}$, respectively.

For illustration, we give an example of the relevant couplings for the radion [g_{0jk}^{LL} , g_{0jk}^{RR} and $m_{0jk}^{LR}/k_{\text{eff}} e^{-A(L)}$] and for the KK-radion [g_{1jk}^{LL} , g_{1jk}^{RR} and $m_{1jk}^{LR}/k_{\text{eff}} e^{-A(L)}$], to the lowest lying KK fermions. In Table 1 we give the couplings in the “strong warping” benchmark scenario, while Table 2 contains the corresponding couplings in the “small warping” benchmark scenario (these scenarios are defined in Subsection 2.3.3). We chose $c = -0.2$, as might be appropriate for the $SU(2)$ top singlet. In this case, the fermion masses are given by $m_n = x_n^f e^{-A(L)}$, with $x_n^f = 0, 1.15, 3.38, 4.32, 6.50, 7.43, \dots$ ($x_n^f = 0, 0.97, 2.96, 3.78, 5.63, 6.51, \dots$) in the strong (small) warping benchmark scenarios. Even (odd) n correspond to KK-parity even (odd) states. For such c -values, the KK-parity even and odd states are not as degenerate as for $c = 1/2$, but one can recognize the corresponding semi-degenerate pairs. Note that the tables display the selection rules implied by KK-parity conservation. We also point out that the last integral in the definition of m_{ijk}^{RL} [see Eq. (97)] typically gives a small contribution, although it has been included in the numerical evaluation of Tables 1 and 2. We see in the tables that the couplings involving fermions other than the zero-mode and/or the first (“ultra-light”) fermion excitation, are almost vector-like (see the 4×4 submatrices in the lower right corner of each table). The couplings involving t and t' , on the other hand, are close to chiral, as we have also exhibited in Eqs. (106) and (107).

7.2 KK-Radion Couplings to Gauge Bosons and the Higgs Fields

We also summarize the Feynman rules for one or two radion KK modes and two gauge KK modes. We focus on the interactions with V_μ^n , which are sufficient for tree-level calculations (where one can work in unitary gauge with $V_5^n = 0$). The $F_{\mu\nu} F^{\mu\nu}$ terms in Eq. (90) give

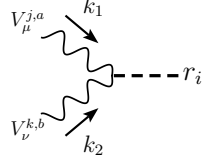
$$-\frac{1}{4} \frac{1}{2L} \sum_{j,k=0}^{\infty} [1 + 2F(x, y)] f_V^j f_V^k F_{\mu\nu}^j(x) F^{\mu\nu k}(x), \quad (108)$$

(with indices raised by the Minkowski metric), while the $F_{\mu 5} F^{\mu 5}$ terms give

$$\frac{1}{2} \frac{1}{2L} \sum_{j,k=0}^{\infty} e^{-2[A(y)+F(x,y)]} [1 + 2F(x, y)]^{-1} \partial_y f_V^j \partial_y f_V^k V_\mu^j(x) V^{\mu k}(x), \quad (109)$$

where we used the parameterization of the radion modes given in Eq. (29), as well as the gauge KK decomposition, Eq. (92). Using also the radion KK decomposition of Eq. (32),

with $r_i(x) \equiv \Lambda_r \tilde{r}_i(x)$, the Feynman rule for the vertex involving a single radion and two gauge fields reads

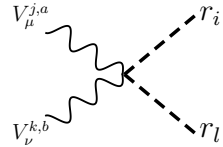


$$= \frac{2i}{\Lambda_r} \delta^{ab} \left\{ g_{ijk} [k_1 \cdot k_2 \eta_{\mu\nu} - k_{1\mu} k_{2\nu}] - 2g_{ijk}^m m_j m_k \eta_{\mu\nu} \right\} , \quad (110)$$

where

$$g_{ijk} = \frac{1}{2L} \int_{-L}^L dy F_i f_V^j f_V^k , \quad g_{ijk}^m = \frac{1}{2L} \int_{-L}^L dy e^{-2A} F_i f_5^j f_5^k , \quad (111)$$

and we restored the gauge indices, a, b . Here we used $f_5^j = \partial_y f_V^j / m_j$, since it is simpler to find $f_5^j(y)$ numerically.²¹ Note that Eqs. (111) with $F_i \rightarrow 1$ are precisely the orthonormality relations for the f_V^j and f_5^j . For completeness, we also quote the interactions of two radions and two gauge bosons, which arise from Eq. (109), although these do not involve the gauge zero-modes:



$$= \frac{20i}{\Lambda_r^2} \delta^{ab} g_{iljk}^m m_j m_k \eta_{\mu\nu} , \quad (112)$$

where g_{iljk}^m is defined as g_{ijk}^m in Eq. (111), but with two radion wavefunctions, $F_i F_l$.

Finally, we give the Feynman rules for the Higgs interactions with one and two radion modes. Here we assume, for simplicity, that the Higgs fields are IR localized, so that the radion couplings enter through the induced metric. We also neglect the possible mixing between Higgses and radion modes. Referring to the discussion of kinetic and potential Higgs terms of Subsection 5.1, one must only remember that the radion modes enter through a multiplicative factor $e^{-2F(x,y)}$ when coupled to scalar kinetic terms, and through $e^{-4F(x,y)}$ when coupled to potential terms. Using the radion KK decomposition, Eq. (32), and in terms of the Higgs mass eigenstates defined in Eq. (81), the Feynman rules involving a single radion mode are

$$r_i \phi \phi \longrightarrow i \left[1 + (-1)^i \right] \frac{F_i(L)}{\Lambda_r} [k_1 \cdot k_2 + 2m_\phi^2] , \quad (113)$$

$$r_i h_+ h_- \longrightarrow i \left[1 - (-1)^i \right] \frac{F_i(L)}{\Lambda_r} [k_1 \cdot k_2 + 4m_{h_+}^2] , \quad (114)$$

$$r_i (a, G^0) / (H^\pm G^\mp) \longrightarrow i \left[1 - (-1)^i \right] \frac{F_i(L)}{\Lambda_r} k_1 \cdot k_2 , \quad (115)$$

²¹More concretely, in order to find the gauge KK spectrum, m_j , we apply the ‘‘shooting method’’ described at the end of Subsection 4.1 to $\tilde{f}_5^j \equiv e^{-2A} f_5^j$, which –from Eq. (93)– obeys $\partial_y^2 \tilde{f}_5^j + m_j^2 e^{2A} \tilde{f}_5^j = 0$ and $\tilde{f}_5^j|_{\pm L} = 0$.

where $\phi = h_+, h_-, a, H^\pm, G^0, G^\pm$ (and $m_{G^0, G^\pm}^2 = 0$). We also denoted the (incoming) Higgs momenta by k_1 and k_2 , and $F_i(y)$ is the r_i wavefunction. The Feynman rules involving two radion modes are

$$r_i r_j \phi \phi \longrightarrow -2i [1 + (-1)^{i+j}] \frac{F_i(L) F_j(L)}{\Lambda_r^2} [k_1 \cdot k_2 + 4m_\phi^2] , \quad (116)$$

$$r_i r_j h_+ h_- \longrightarrow -2i [1 - (-1)^{i+j}] \frac{F_i(L) F_j(L)}{\Lambda_r^2} [k_1 \cdot k_2 + 8m_{h_+}^2] , \quad (117)$$

$$r_i r_j (a, G^0)/(H^\pm G^\mp) \longrightarrow -2i [1 - (-1)^{i+j}] \frac{F_i(L) F_j(L)}{\Lambda_r^2} k_1 \cdot k_2 . \quad (118)$$

8 Summary and Conclusions

In this work we have introduced a 5-dimensional scenario where the dynamics that stabilizes the size of the fifth dimension: i) induces the non-trivial warping that allows understanding the weakness of the gravitational interactions compared to the weak interactions ii) leads to a metric background that implies the existence of a KK-parity symmetry, thus predicting a weak scale stable particle (the LKP), iii) leads to fermion localization via Yukawa interactions involving the stabilizing field, and iv) the Higgs sector is described by a THDM with an “inert” Higgs doublet ($\tan \beta = \infty$). It is argued that generically the LKP is the first excitation associated with the radion field. This KK-radion is expected to be highly degenerate with the radion, and its interactions are controlled by the same decay constant that controls the radion interactions. This allows to infer properties of the KK-radion from collider signatures of the radion, and help identify the collider KK-radion signatures. In particular, it may be possible to probe whether the LKP accounts for the DM content of the universe via collider measurements. Although we have not explored this question in this paper (we present the analysis in the companion paper [29]), we have presented the technical ingredients necessary to study the phenomenology of such scenarios. In particular, we provided simple analytical expressions for the masses and wavefunctions of the lowest lying KK states, which can be summarized as follows:

- The KK scale is set by the warped down IR curvature scale, $\tilde{k}_{\text{eff}} = k_{\text{eff}} e^{-A(L)} = A'(L) e^{-A(L)}$, where $2L$ is the proper size of the extra dimension, while $A(y)$ depends on the stabilization mechanism (and needs not be linear in y , as is the case of AdS₅).
- The radion (KK-radion) is strongly and symmetrically (antisymmetrically) localized near the IR boundaries, according to $F_0(y) \approx e^{2[A(y)-A(L)]}$ for $y \in [0, L]$. Their masses are exponentially degenerate at tree level, and given approximately by $\frac{2}{\sqrt{k_{\text{eff}} L}} \tilde{k}_{\text{eff}}$ in the case that the dynamical “UV brane” is fat [see Eq. (43) for a completely general expression].
- The zero-mode fermions have wavefunctions that behave like $e^{-(c-\frac{1}{2})A(y)}$ in the “fat UV brane” limit [see Eqs. (62) and (74), and Eq. (59) for the exact expression in a

general 4D Lorentz invariant background]. The effective c -parameter allows a simple characterization of the localization properties. In the “fat UV brane” limit, UV localized wavefunctions ($c \gtrsim 1/2$) are Gaussian-like, while IR localized wavefunctions ($c \lesssim 1/2$) are approximately exponential.

- The lightest KK fermion excitations that are localized towards the IR boundaries have a mass approximately given by $m_1 \approx \sqrt{2(1+2c)} \tilde{k}_{\text{eff}}$ when $-1/2 \lesssim c \lesssim 1/2$. Their LH and RH wavefunctions were given in Eqs. (72) and (73).

We also provided sample KK spectra and couplings between radion/KK-radion and fermion/gauge modes in Tables 1 and 2, and briefly discussed the fermion couplings to the Higgs, as well as the KK-radion/Higgs interactions. These ingredients are relevant when studying the phenomenology of the present scenario. We discussed the possibility that the curvature scale ranges from order the fundamental Planck scale down to much smaller values. The former case is similar in spirit to the RS proposal, while the latter has some features in common with Universal Extra Dimensions, but allows a consistent description of the gravitational interactions and, via the AdS/CFT correspondence may be a valid description up to a scale exponentially larger than the weak scale (but well below the 4D Planck mass). This latter scenario may allow for a lighter spectrum of KK states than is expected in RS models. The EW and flavor constraints deserve a more detailed study, as does the associated collider phenomenology of the Z_2 -symmetric warped scenarios.

Acknowledgments

We would like to thank Thomas Flacke and especially Arjun Menon for collaboration at early stages of this work. We also thank Hsin-Chia Cheng for discussions. A.M. is supported by the US department of Energy under contract DE-FG02-91ER406746. E.P. is supported by DOE grant DE-FG02-92ER40699.

References

- [1] L. Randall and R. Sundrum, Phys. Rev. Lett. **83**, 3370 (1999) [arXiv:hep-ph/9905221].
- [2] H. Davoudiasl, J. L. Hewett and T. G. Rizzo, Phys. Lett. B **473**, 43 (2000) [arXiv:hep-ph/9911262];
- [3] A. Pomarol, Phys. Lett. B **486**, 153 (2000) [arXiv:hep-ph/9911294].
- [4] Y. Grossman and M. Neubert, Phys. Lett. B **474**, 361 (2000) [arXiv:hep-ph/9912408].
- [5] T. Gherghetta and A. Pomarol, Nucl. Phys. B **586** (2000) 141 [arXiv:hep-ph/0003129].
- [6] R. Sundrum, Phys. Rev. D **59**, 085010 (1999) [arXiv:hep-ph/9807348].

- [7] N. Arkani-Hamed, S. Dimopoulos and J. March-Russell, Phys. Rev. D **63**, 064020 (2001) [arXiv:hep-th/9809124].
- [8] W. D. Goldberger, M. B. Wise, Phys. Rev. Lett. **83**, 4922-4925 (1999). [hep-ph/9907447].
- [9] J. Garriga, O. Pujolas and T. Tanaka, Nucl. Phys. B **605**, 192 (2001) [arXiv:hep-th/0004109].
- [10] W. D. Goldberger and I. Z. Rothstein, Phys. Lett. B **491**, 339 (2000) [arXiv:hep-th/0007065].
- [11] J. Garriga and A. Pomarol, Phys. Lett. B **560**, 91 (2003) [arXiv:hep-th/0212227].
- [12] Y. Bai, M. Carena and E. Pontón, Phys. Rev. D **81**, 065004 (2010) [arXiv:0809.1658 [hep-ph]].
- [13] N. Maru and Y. Sakamura, JHEP **1004**, 100 (2010) [arXiv:1002.4259 [hep-ph]].
- [14] H. Davoudiasl and E. Pontón, JHEP **1010**, 102 (2010) [arXiv:1007.2672 [hep-ph]].
- [15] W. D. Goldberger and M. B. Wise, Phys. Lett. B **475**, 275 (2000) [arXiv:hep-ph/9911457].
- [16] C. Csaki, M. L. Graesser and G. D. Kribs, Phys. Rev. D **63**, 065002 (2001) [arXiv:hep-th/0008151].
- [17] T. G. Rizzo, JHEP **0206**, 056 (2002) [arXiv:hep-ph/0205242].
- [18] C. Csaki, J. Hubisz and S. J. Lee, Phys. Rev. D **76**, 125015 (2007) [arXiv:0705.3844 [hep-ph]].
- [19] C. Csaki, M. Graesser, L. Randall and J. Terning, Phys. Rev. D **62**, 045015 (2000) [arXiv:hep-ph/9911406].
- [20] G. F. Giudice, R. Rattazzi and J. D. Wells, Nucl. Phys. B **595**, 250 (2001) [arXiv:hep-ph/0002178].
- [21] D. Dominici, B. Grzadkowski, J. F. Gunion and M. Toharia, Nucl. Phys. B **671**, 243 (2003) [arXiv:hep-ph/0206192]. J. F. Gunion, M. Toharia and J. D. Wells, Phys. Lett. B **585**, 295 (2004) [arXiv:hep-ph/0311219].
- [22] K. Agashe, A. Falkowski, I. Low and G. Servant, JHEP **0804**, 027 (2008) [arXiv:0712.2455 [hep-ph]].
- [23] H. Davoudiasl, S. Gopalakrishna, E. Pontón and J. Santiago, New J. Phys. **12**, 075011 (2010) [arXiv:0908.1968 [hep-ph]].

- [24] T. Appelquist, H. -C. Cheng, B. A. Dobrescu, Phys. Rev. **D64**, 035002 (2001). [hep-ph/0012100].
- [25] B. A. Dobrescu and E. Pontón, JHEP **0403**, 071 (2004) [arXiv:hep-th/0401032]; G. Burdman, B. A. Dobrescu and E. Pontón, JHEP **0602**, 033 (2006) [arXiv:hep-ph/0506334].
- [26] K. L. McDonald, Phys. Rev. D **80**, 024038 (2009) [arXiv:0905.3006 [hep-ph]].
- [27] H. C. Cheng, K. T. Matchev and M. Schmaltz, Phys. Rev. D **66**, 036005 (2002) [arXiv:hep-ph/0204342].
- [28] E. Pontón and L. Wang, JHEP **0611**, 018 (2006) [arXiv:hep-ph/0512304].
- [29] A. D. Medina and E. Pontón, arXiv:1104.4124 [hep-ph].
- [30] S. S. Gubser, Adv. Theor. Math. Phys. **4**, 679 (2000) [arXiv:hep-th/0002160].
- [31] A. Karch, E. Katz, D. T. Son and M. A. Stephanov, Phys. Rev. D **74**, 015005 (2006) [arXiv:hep-ph/0602229]. B. Batell and T. Gherghetta, Phys. Rev. D **78**, 026002 (2008) [arXiv:0801.4383 [hep-ph]].
- [32] A. Falkowski and M. Perez-Victoria, JHEP **0812**, 107 (2008) [arXiv:0806.1737 [hep-ph]]; A. Falkowski and M. Perez-Victoria, Phys. Rev. D **79**, 035005 (2009) [arXiv:0810.4940 [hep-ph]].
- [33] B. Batell, T. Gherghetta and D. Sword, Phys. Rev. D **78**, 116011 (2008) [arXiv:0808.3977 [hep-ph]]. T. Gherghetta and D. Sword, Phys. Rev. D **80**, 065015 (2009) [arXiv:0907.3523 [hep-ph]]. T. Gherghetta and N. Setzer, Phys. Rev. D **82**, 075009 (2010) [arXiv:1008.1632 [hep-ph]].
- [34] A. Delgado and D. Diego, Phys. Rev. D **80**, 024030 (2009) [arXiv:0905.1095 [hep-ph]].
- [35] S. Mert Aybat and J. Santiago, Phys. Rev. D **80**, 035005 (2009) [arXiv:0905.3032 [hep-ph]].
- [36] J. A. Cabrer, G. von Gersdorff and M. Quirós, New J. Phys. **12**, 075012 (2010) [arXiv:0907.5361 [hep-ph]].
- [37] M. Atkins and S. J. Huber, Phys. Rev. D **82**, 056007 (2010) [arXiv:1002.5044 [hep-ph]].
- [38] G. von Gersdorff, Phys. Rev. D **82**, 086010 (2010) [arXiv:1005.5134 [hep-ph]].
- [39] J. A. Cabrer, G. von Gersdorff and M. Quiros, Phys. Lett. B **697**, 208 (2011) [arXiv:1011.2205 [hep-ph]].
- [40] Y. Bai, G. Burdman and C. T. Hill, JHEP **1002**, 049 (2010) [arXiv:0911.1358 [hep-ph]].

- [41] C. T. Hill and R. J. Hill, Phys. Rev. D **76**, 115014 (2007) [arXiv:0705.0697 [hep-ph]].
- [42] D. Z. Freedman, S. S. Gubser, K. Pilch and N. P. Warner, Adv. Theor. Math. Phys. **3**, 363 (1999) [arXiv:hep-th/9904017].
- [43] A. Brandhuber and K. Sfetsos, JHEP **9910**, 013 (1999) [arXiv:hep-th/9908116].
- [44] O. DeWolfe, D. Z. Freedman, S. S. Gubser and A. Karch, Phys. Rev. D **62**, 046008 (2000) [arXiv:hep-th/9909134].
- [45] Z. Chacko, M. A. Luty and E. Pontón, JHEP **0007**, 036 (2000) [arXiv:hep-ph/9909248].
- [46] N. Arkani-Hamed and M. Schmaltz, Phys. Rev. D **61**, 033005 (2000) [arXiv:hep-ph/9903417].
- [47] D. E. Kaplan, T. M. P. Tait, JHEP **0111**, 051 (2001). [hep-ph/0110126].
- [48] H. Davoudiasl, J. L. Hewett and T. G. Rizzo, Phys. Rev. D **68**, 045002 (2003) [arXiv:hep-ph/0212279]; M. S. Carena, E. Pontón, T. M. P. Tait and C. E. M. Wagner, Phys. Rev. D **67**, 096006 (2003) [arXiv:hep-ph/0212307].
- [49] L. Randall, M. D. Schwartz, JHEP **0111**, 003 (2001). [hep-th/0108114].

$\mathbf{g}_{0jk}^{\text{LL}}$							$\mathbf{g}_{1jk}^{\text{LL}}$						
x_n^f	0	1.15	3.38	4.32	6.50	7.43	0	1.15	3.38	4.32	6.50	7.43	
0	0	0	0	0	0	0	0	0	0	0	0	0	
1.15	0	0.08	0	0.13	0	0.02	0	0	0.15	0	0.05	0	
3.38	0	0	0.30	0	0.18	0	0	0.15	0	0.29	0	0.12	
4.32	0	0.13	0	0.31	0	0.19	0	0	0.29	0	0.24	0	
6.50	0	0	0.18	0	0.32	0	0	0.05	0	0.24	0	0.31	
7.43	0	0.02	0	0.19	0	0.32	0	0	0.12	0	0.31	0	

$\mathbf{g}_{0jk}^{\text{RR}}$							$\mathbf{g}_{1jk}^{\text{RR}}$						
x_n^f	0	1.15	3.38	4.32	6.50	7.43	0	1.15	3.38	4.32	6.50	7.43	
0	0.41	0	0.29	0	0.08	0	0	0.46	0	0.20	0	0.06	
1.15	0	0.52	0	0.26	0	0.08	0.46	0	0.35	0	0.11	0	
3.38	0.29	0	0.35	0	0.22	0	0	0.35	0	0.33	0	0.16	
4.32	0	0.26	0	0.34	0	0.21	0.20	0	0.33	0	0.27	0	
6.50	0.08	0	0.22	0	0.34	0	0	0.11	0	0.27	0	0.32	
7.43	0	0.08	0	0.21	0	0.33	0.06	0	0.16	0	0.32	0	

$\mathbf{m}_{0jk}^{\text{LR}}/\tilde{k}_{\text{eff}}$							$\mathbf{m}_{1jk}^{\text{LR}}/\tilde{k}_{\text{eff}}$						
x_n^f	0	1.15	3.38	4.32	6.50	7.43	0	1.15	3.38	4.32	6.50	7.43	
0	0	0	0	0	0	0	0	0	0	0	0	0	
1.15	0	1.45	0	1.68	0	0.52	1.12	0	1.78	0	0.86	0	
3.38	2.05	0	4.43	0	3.78	0	0	2.80	0	4.77	0	2.89	
4.32	0	2.67	0	5.67	0	4.57	1.88	0	4.91	0	5.45	0	
6.50	1.09	0	4.18	0	8.56	0	0	1.64	0	5.73	0	8.74	
7.43	0	1.27	0	4.90	0	9.79	0.87	0	3.33	0	8.83	0	

\mathbf{g}_{1jk}						$\mathbf{g}_{1jk}^{\text{m}}$				
x_n^V	0	2.39	2.41	5.46	5.49	0	2.39	2.41	5.46	5.49
0	0	0.06	0	0.01	0	0	0	0	0	0
2.39	0.06	0	0.56	0	0.24	0	0	0.22	0	0.17
2.41	0	0.56	0	0.24	0	0	0.22	0	0.17	0
5.46	0.01	0	0.24	0	0.37	0	0	0.17	0	0.31
5.49	0	0.24	0	0.37	0	0	0.17	0	0.31	0

Table 1: Radion (left) and KK-radion (right) couplings to KK fermion pairs [see Eq. (95)] in the “strong warping scenario”, for $c = -0.2$. We also show the KK-radion-gauge boson couplings [see Eq. (111)]. The lowest lying KK fermion masses, in units of $\tilde{k}_{\text{eff}} = k_{\text{eff}} e^{-A(L)}$, are $x_0^f = 0$, $x_1^f \approx 1.15$, $x_2^f \approx 3.38$, $x_3^f \approx 4.32$, $x_4^f \approx 6.50$ and $x_5^f \approx 7.43$, while the gauge boson ones are $x_0^V = 0$, $x_1^V \approx 2.39$, $x_2^V \approx 2.41$, $x_3^V \approx 5.46$ and $x_4^V \approx 5.49$. The states with mass x_n with even (odd) n are KK-parity even (odd). In general, EWSB will lift x_0 to a non-vanishing value. The radion and KK-radion masses are $m_0 \approx m_1 \approx 0.22 \tilde{k}_{\text{eff}}$. The dimensionless values in this table were computed assuming $\tilde{k} = 2$ TeV (which corresponds to $\tilde{k}_{\text{eff}} \approx 1.2$ TeV), but are rather insensitive to this choice, as long as $\tilde{k} \sim \mathcal{O}(\text{TeV})$.

$\mathbf{g}_{0jk}^{\text{LL}}$							$\mathbf{g}_{1jk}^{\text{LL}}$						
x_n^f	0	0.97	2.96	3.78	5.63	6.51	0	0.97	2.96	3.78	5.63	6.51	
0	0	0	0	0	0	0	0	0	0	0	0	0	
0.97	0	0.06	0	0.11	0	0.03	0	0	0.11	0	0.05	0	
2.96	0	0	0.24	0	0.17	0	0	0.11	0	0.25	0	0.13	
3.78	0	0.11	0	0.27	0	0.18	0	0	0.25	0	0.22	0	
5.63	0	0	0.17	0	0.27	0	0	0.05	0	0.22	0	0.27	
6.51	0	0.03	0	0.18	0	0.28	0	0	0.13	0	0.27	0	

$\mathbf{g}_{0jk}^{\text{RR}}$							$\mathbf{g}_{1jk}^{\text{RR}}$						
x_n^f	0	0.97	2.96	3.78	5.63	6.51	0	0.97	2.96	3.78	5.63	6.51	
0	0.38	0	0.28	0	0.10	0	0	0.42	0	0.22	0	0.07	
0.97	0	0.48	0	0.26	0	0.09	0.42	0	0.33	0	0.13	0	
2.96	0.28	0	0.32	0	0.21	0	0	0.33	0	0.30	0	0.16	
3.78	0	0.26	0	0.31	0	0.21	0.22	0	0.30	0	0.25	0	
5.63	0.10	0	0.21	0	0.29	0	0	0.13	0	0.25	0	0.28	
6.51	0	0.09	0	0.21	0	0.30	0.07	0	0.16	0	0.28	0	

$\mathbf{m}_{0jk}^{\text{LR}}/\tilde{k}_{\text{eff}}$							$\mathbf{m}_{1jk}^{\text{LR}}/\tilde{k}_{\text{eff}}$						
x_n^f	0	0.97	2.96	3.78	5.63	6.51	0	0.97	2.96	3.78	5.63	6.51	
0	0	0	0	0	0	0	0	0	0	0	0	0	
0.97	0	1.06	0	1.31	0	0.58	0.84	0	1.31	0	0.82	0	
2.96	1.70	0	3.34	0	3.17	0	0	2.22	0	3.68	0	2.59	
3.78	0	2.24	0	4.40	0	3.87	1.67	0	3.78	0	4.40	0	
5.63	1.14	0	3.43	0	6.38	0	0	1.59	0	4.56	0	6.66	
6.51	0	1.28	0	4.09	0	7.59	0.93	0	2.91	0	6.71	0	

\mathbf{g}_{1jk}						$\mathbf{g}_{1jk}^{\text{m}}$				
x_n^V	0	2.19	2.41	4.86	5.17	0	2.19	2.41	4.86	5.17
0	0	0.16	0	0.04	0	0	0	0	0	0
2.19	0.16	0	0.51	0	0.22	0	0	0.19	0	0.15
2.41	0	0.51	0	0.26	0	0	0.19	0	0.18	0
4.86	0.04	0	0.26	0	0.33	0	0	0.18	0	0.27
5.17	0	0.22	0	0.33	0	0	0.15	0	0.27	0

Table 2: Radion (left) and KK-radion (right) couplings to KK fermion pairs [see Eq. (95)] in the “small warping scenario”, for $c = -0.2$. We also show the KK-radion-gauge boson couplings [see Eq. (111)]. The lowest lying KK fermion masses, in units of $\tilde{k}_{\text{eff}} = k_{\text{eff}} e^{-A(L)}$, are $x_0^f = 0$, $x_1^f \approx 0.97$, $x_2^f \approx 2.96$, $x_3^f \approx 3.78$, $x_4^f \approx 5.63$ and $x_5^f \approx 6.51$, while the gauge boson ones are $x_0^V = 0$, $x_1^V \approx 2.19$, $x_2^V \approx 2.41$, $x_3^V \approx 4.86$ and $x_4^V \approx 5.17$. The states with mass x_n with even (odd) n are KK-parity even (odd). In general, EWSB will lift x_0 to a non-vanishing value. The radion and KK-radion masses are $m_0 \approx m_1 \approx 0.66 \tilde{k}_{\text{eff}}$. The dimensionless values in this table were computed assuming $\tilde{k} = 2 \text{ TeV}$ (which corresponds to $\tilde{k}_{\text{eff}} \approx 500 \text{ GeV}$), but are not very sensitive to this choice, as long as $\tilde{k} \sim \mathcal{O}(\text{TeV})$.